https://doi.org/10.5194/egusphere-2026-4192
Preprint. Discussion started: 17 July 2026

Arctic phytoplankton bloom regimes are associated with distinct dissolved carbohydrate signatures and transparent exopolymer particle (TEP) formation

Sophia Hirschmann[1], Anabel von Jackowski[1,2], Benjamin Pontiller[1], Katja Metfies[3], Vasily Povazhnyi[4], Stefan Neuhaus[3], Eva-Maria Nöthig[3], Anja Engel[1]

[1]Marine Biogeochemistry, GEOMAR Helmholtz Centre for Ocean Research, Kiel, Germany
[2]Stockholm University, Stockholm, Sweden
[3]Alfred Wegener Institute, Helmholtz Centre for Polar and Marine Research, Bremerhaven, Germany
[4]Arctic and Antarctic Research Institute, St. Petersburg, Russia

Correspondence to: Sophia Hirschmann (s.hirschmann@gmx.net); Anja Engel (aengel@geomar.de)

Short summary (500 character)

Phytoplankton release dissolved organic carbon, including carbohydrates, which are either recycled by microbes or form sticky, sugar-containing gels that may contribute to carbon export via aggregation. By studying phytoplankton communities, dissolved carbohydrate composition and gel formation in the Fram Strait and Kara Sea, we show that blooms dominated by different phytoplankton groups leave distinct organic signatures, suggesting that community shifts could alter carbon processing pathways.

Abstract. Phytoplankton are major producers of marine dissolved organic matter (DOM), including carbohydrates that fuel microbial carbon cycling or contribute to the biological carbon pump through exopolymer particle aggregation. In the Arctic Ocean, climate-driven changes are expected to restructure phytoplankton communities, yet the consequences for the molecular composition of DOM and its fate within microbial and aggregation pathways remain unclear. Here, we examined potential linkages between phytoplankton community composition (18S-rRNA), dissolved organic carbon (DOC), dissolved combined carbohydrates (DCCHO) and transparent exopolymer particles (TEP) in the Fram Strait and the Kara Sea. An advanced spring bloom dominated by the haptophyte *Phaeocystis pouchetii* coincided with a DOM pool enriched in neutral and acidic carbohydrates and elevated TEP concentrations. In contrast, ice-edge diatom blooms dominated by *Thalassiosira* spp. were characterized by glucose-enriched DOM signatures and low TEP formation. Our findings indicate an association between specific phytoplankton taxa and exopolymeric carbohydrate composition, suggesting that shifts in phytoplankton biodiversity may alter carbon processing pathways.

https://doi.org/10.5194/egusphere-2026-4192
Preprint. Discussion started: 17 July 2026

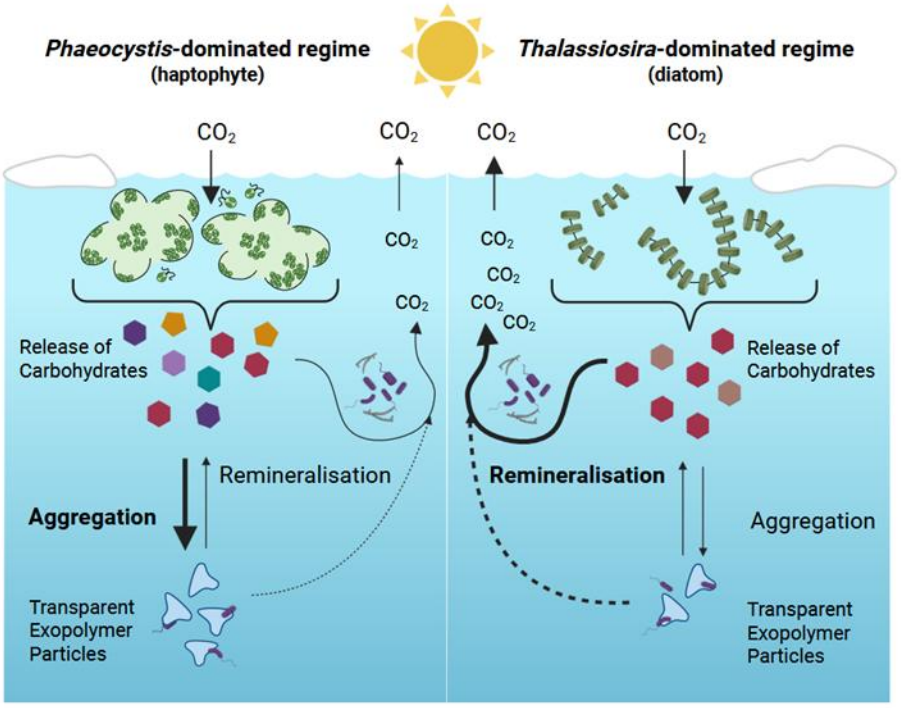

Contrasting phytoplankton blooms produce distinct carbohydrate signatures (hexagons: red, glucose; brown, mannose+xylose; yellow, arabinose; dark purple, rhamnose; lilac, galacturonic acid; cyan, glucuronic acid), with implications for carbon processing pathways, either promoting transparent exopolymer particle (TEP, light blue triangles) formation or coinciding with lower TEP formation and suggesting enhanced remineralization.

1 Introduction

Marine phytoplankton account for roughly half of global primary production and form the base of oceanic food webs by converting inorganic carbon into organic matter (Falkowski et al., 1998). A fraction of this production, typically 5-45% depending on species, growth phase, and environmental conditions, is released as dissolved organic matter (DOM) (Fogg, 1966, Prakash et al., 2024). DOM release occurs passively through leakage across cell membranes or actively via exudation associated with waste removal, substrate acquisition, communication, or defence (Sharp, 1977; Bjørrisen, 1988; Thornton, 2014). Top-down processes, including sloppy feeding by zooplankton and protists as well as viral lysis, release additional cellular material into the organic matter pool (Strom et al., 1997; Møller, 2007; Lønborg et al., 2013). DOM is a complex mixture of organic molecules that contains substantial amounts of dissolved organic carbon (DOC) and represents one of Earth's largest exchangeable carbon reservoirs, similar in scale to atmospheric CO_2 (Hansell et al., 2009; Hedges, 1992). Carbohydrates represent a major fraction of the marine DOM pool and phytoplankton-derived organic matter (Biersmith &

https://doi.org/10.5194/egusphere-2026-4192
Preprint. Discussion started: 17 July 2026

Benner, 1998; Kaiser & Benner, 2009; Borchard & Engel, 2012; Sperling et al., 2017). By releasing a diverse suite of organic compounds, phytoplankton shape both the molecular composition and quantity of DOM, which in turn control its bioavailability and turnover, and consequently the fate of organic carbon in the water column (Kieft et al., 2021; Vidal-Melgosa et al., 2021).

Phytoplankton-derived DOC is removed from the surface ocean via two main pathways with contrasting implications for carbon cycling: it is either rapidly remineralized by heterotrophic microbes, resulting in fast recycling and CO_2 exchange with the atmosphere, or transformed into particulate organic carbon aggregation processes with implications for carbon export. Most freshly released DOC is metabolised by heterotrophic microbes (Coffin et al., 1993; Carlson et al., 1999) or transferred to higher trophic levels; however, excess DOC can accumulate in surface waters during or towards the end of a phytoplankton bloom and promote the formation of gel-like particles (Azam 1998; Mari 1999; Passow 2000). Marine gel particles, such as polysaccharide-containing transparent exopolymer particles (TEP), can assemble from dissolved precursors (e.g., acidic sugars), which comprise between 5-40% of DOM (Pakulski & Benner, 1994; Engel et al., 2004a). Due to their sticky properties, TEP play an important role in the formation and sedimentation of larger aggregates, thereby linking dissolved and particulate organic matter pools and facilitating vertical carbon export (Engel, 2000; Engel et al., 2004b; Verdugo et al., 2004).

The influence of environmental conditions on the production and release of phytoplankton-derived DOM has been widely investigated, with experimental studies showing that factors such as nutrient and light availability, CO_2 concentration, and temperature affect both its quantity and composition (Granum et al., 2002; Borchard & Engel, 2012; Toseland 2013). In parallel, culture experiments have demonstrated that different phytoplankton taxa release distinct suites of organic compounds, suggesting a taxonomic imprint on DOM composition (Aluwihare & Repeta, 1999; Urbani et al., 2005; Eigemann et al., 2023). For example, Becker et al. (2014) showed that closely related phytoplankton species produce DOM with similar molecular characteristics. Yet, it remains unclear to what extent such taxon-specific signatures are preserved in natural marine systems, and how shifts in phytoplankton community composition might affect the balance between microbial recycling and the aggregation-driven carbon export.

The Arctic Ocean is particularly affected by ongoing environmental change (Rantanen et al., 2022). In the Eurasian Arctic, the northward expansion of warmer, saltier Atlantic waters into the Arctic Basin - termed Atlantification - and increasing freshwater input from Eurasian rivers are altering stratification, heat distribution, and nutrient regimes (Peterson et al., 2002; McClelland et al., 2006; Tesi et al., 2021). In the Greenland sector, the Fram Strait (FS) serves as the only deep gateway between the Arctic and the Atlantic Ocean, where southward-flowing cold, fresh, mostly ice-covered polar waters (PW) carried by the East Greenland Current (EGC) converge with northward-flowing warm, nutrient-rich Atlantic waters (AW) transported by the West Spitsbergen Current (WSC) (Rudels 2009). The resulting strong gradients between PW and AW create a highly dynamic and productive Marginal Ice Zone (MIZ) (Gradinger & Baumann, 1991; v. Appen et al., 2018) and structure phytoplankton assemblages across the strait (Nöthig et al., 2015). In contrast, the Kara Sea (KS) is a shallow Siberian shelf sea that, while also influenced by modified Atlantic waters entering from both the Fram Strait (FSAW) and the Barents Sea (BSAW) (Schauer et al., 2002; Osadchiev et al., 2022; Pérez-Tribouillier et al., 2025), is strongly shaped by riverine input.

https://doi.org/10.5194/egusphere-2026-4192
Preprint. Discussion started: 17 July 2026

The KS receives more than 40% of the total Arctic river runoff, primarily from the Ob and the Yenisei rivers. Together they deliver large amounts of terrestrial organic matter and nutrients (Ivanov, 1976; Gordeev et al.,1996;), supporting roughly one-third of total Arctic primary production (Pivovarov et al., 2003; Terhaar et al., 2021).

Shifts in phytoplankton community composition are already being reported in both the Fram Strait (Ingvaldsen et al., 2021; Ahme et al., 2023; Xi et al., 2025) and the Kara Sea (Sergeeva et al., 2025). Concurrently, annual net primary production (NPP) has increased, particularly in shelf regions such as the Kara Sea, where rates rose by up to 112% due to reduced sea ice and longer growing seasons (Arrigo & van Dijken, 2015; Lewis et al., 2020). Future projections estimate pan-Arctic primary production in ice-free waters at 466-1008 Tg C yr^{-1} (Codispoti et al., 2013; Hill et al., 2013), potentially releasing ~163-353 Tg DOC yr^{-1} assuming an exudation rate of 35% (Amon et al., 2024). Together, these changes highlight the need to better understand the extent to which shifts in phytoplankton community composition influence DOM composition, and ultimately, the balance between carbon recycling and sequestration. In this study, we investigated two hydrographically distinct regions of the Arctic Ocean – the Fram Strait and the Kara Sea – combining measurements of organic matter composition with phytoplankton community data derived from 18S rRNA gene amplicons. Specifically, we aimed to: i) assess regional differences in DOM quantity and quality across hydrographic regimes, ii) examine the potential influence of phytoplankton community structure on the composition of dissolved combined carbohydrates (DCCHO) and TEP concentration.

2. Material and Methods

2.1 Study Sites and Sampling Strategy

In 2021, we conducted sampling campaigns in the Fram Strait onboard the RV *Polarstern* (PS126) from 24 May to 27 June and in the Kara Sea onboard the RV *Akademik Tryoshnikov* (Arctic Century/AT21) from 5 August to 6 September (Fig. 1). We collected samples from 19 CTD/Rosette stations within the Long-Term Ecological Research observatory (LTER-HAUSGARTEN) in the Fram Strait (FS), 12 CTD/Rosette stations in the Kara Sea (KS), 11 underway stations and one CTD/Rosette station in the Ob-Yenisei River Plume (RP) (Table S1). Seawater samples for biochemical and microbial analysis were collected from the surface (1.5-10m) and chlorophyll-*a* maximum (10-42m) using a CTD rosette (SBE 911plus, Sea-Bird Scientific, USA) equipped with two temperature sensors, two conductivity sensors and one chlorophyll sensor. Due to the ice conditions during AT21 expedition, some samples could only be collected from the ship's underway system (~8 m depth), with temperature and salinity measurements taken in a bucket for 30 seconds using an underwater CTD system (UCTD). The full CTD data sets are publicly available on PANGAEA (Hölemann et al, 2022; Makhotin et al., 2022; Tippenhauer et al., 2023).

The data sets of both campaigns were compared by categorically assigning them into a "surface"-layer defined as 0-10 m and "subsurface"-layer for samples taken in 10-42 m (Fig. S1). Based on measured chlorophyll-*a* (chl-*a*) concentrations, two-thirds of the stations displayed a chl-*a* maximum in the subsurface layer, therefore, this layer will be referred to in the

https://doi.org/10.5194/egusphere-2026-4192
Preprint. Discussion started: 17 July 2026

following as the subsurface chlorophyll-*a* maximum layer (SCM). Exceptions included stations without a distinct chl-*a* maximum (S3, SV1, 13, 24, 57) and stations where the maximum was located within the surface layer (EG1, 0Grad, N5, HG5, HG3, 113).

To illustrate the hydrographic conditions during the two expeditions, we generated overview maps of sea surface temperature (SST) for the Fram Strait and the Kara Sea using data from the Copernicus Marine Environment Monitoring Service (CMEMS). Daily data were derived from the Global Ocean OSTIA Sea Surface Temperature and Sea Ice Analysis (SST_GLO_SST_L4_NRT_OBSERVATIONS_010_001; E.U. Copernicus Marine Service Information (CMEMS), Marine Data Store (MDS), DOI: 10.48670/moi-00165, based on Good et al., 2020; Donlon et al., 2012; Stark et al., 2007) and averaged over the respective sampling periods (PS126: 30 May–21 June 2021; AT21: 09 August–03 September 2021). The R packages *tidync* (v0.4.0; Sumner 2024) and *terra* (v1.8-29; Hijmans 2025) were used for processing NetCDF files and creating raster layers, respectively. Visualization and final map preparation were conducted in *QGIS* (v3.34.10; QGIS Development Team 2023). Water mass properties were calculated following the TEOS-10 framework (IOC et al., 2010) using the *gsw* package (v 1.2-0; Kelley et al. 2024) in R.

https://doi.org/10.5194/egusphere-2026-4192
Preprint. Discussion started: 17 July 2026

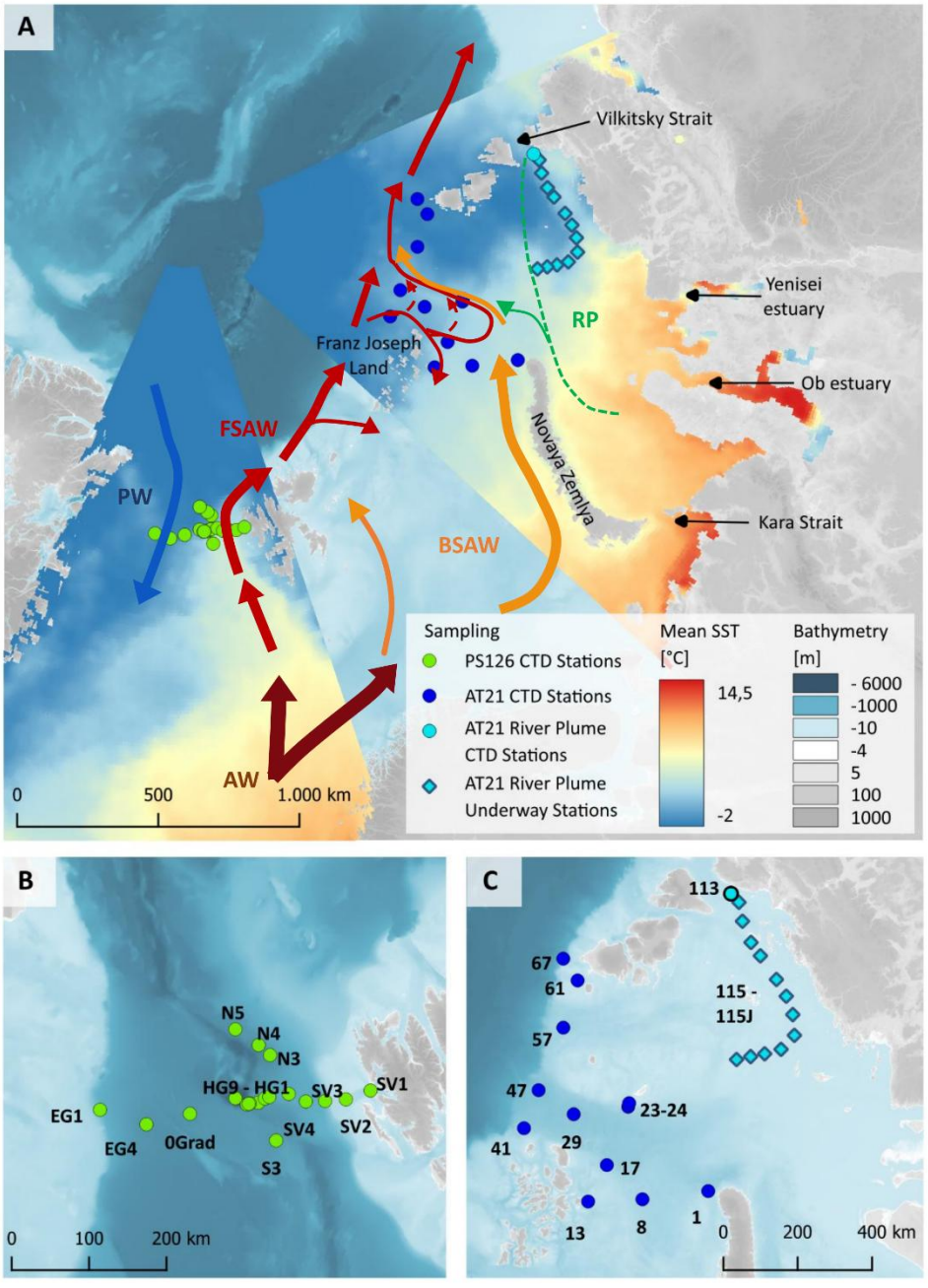

Figure 1: Map of sampled stations during the expeditions PS126 (light green) and AT21 (blue) in summer 2021, with a schematic representation of the intrusion of Atlantic water masses into the Arctic (Atlantic Water (AW) in brown, Fram Strait Atlantic Water (FSAW) in red, Barents Sea Atlantic Water (BSAW) in orange), the outflow of Arctic water through the Fram Strait (Polar Water (PW) in blue) and the extent of the river plume (RP) in the Kara Sea (green dotted line) adapted after Pérez-Tribouillier et al., 2025. Blue to white colours indicate water depth and azure to red colours indicate mean satellite-derived sea surface temperature during the respective sampling period (A). Zoom in on Fram Strait stations and (B) Kara Sea and Ob-Yenisei River Plume stations (C).

https://doi.org/10.5194/egusphere-2026-4192
Preprint. Discussion started: 17 July 2026

2.2 Chlorophyll-a

Chlorophyll-*a* (chl-*a*) concentrations were determined according to Edler (1979) and Evans and O'Reily, (1980) with modifications. In brief, up to 1 L of seawater were filtered onto 25 mm GF/F (Cytiva Whatman™, USA), which were stored at -20°C until analysis. For Fram Strait samples, pigments were extracted using acetone (90%, 2-4 hrs in the dark) and then centrifuged for 10 min at 4°C at 5000 rpm before fluorometric analysis (Turner Designs, USA). For Kara Sea samples, pigments were extracted with acetone (90%) in the dark for 24 h and measured on a pre-calibrated (pure spinach Chl-A, Sigma) fluorometer (Trilogy, Turner Designs, USA) by "no acidification" protocol.

2.3 Inorganic nutrients

During PS126, 10 mL of seawater were filtered in triplicates through 0.8 µm pore-sized cellulose acetate syringe-filters (Thermo Fisher Scientific, US) and stored at -20°C. At the central laboratory for chemical analysis (ZLCA) at GEOMAR, nitrate (NO_3-), nitrite (NO_2-), phosphate (PO_4^{3-}) and silicic acid ($Si(OH)_4$) were quantified on a QuAAtro39 AutoAnalyzer (Seal Analytical Inc., USA) using salinity-adjusted (35 PSU) standards. For AT21, a detailed description of the nutrient analysis can be found in Gangnus et al. (2022).

2.4 Protist community composition analysis

During PS126, up to 6 L of seawater were pre-filtered (10 µm) and size fractionated using 3 µm and 0.4 µm PC filters (Millipore, USA). Filters were stored frozen (-80 °C). During AT21, up to 2 L of seawater were filtered directly onto 0.2 µm Sterivex filter units (Millipore, USA) with 1 mL of RNAlater (Thermo Fisher Scientific, USA) and then stored (-80 °C). Size fractionated samples were pooled after DNA extraction using the NucleoSpin Plant II Kit (Macherey-Nagel, Germany) for PS126 samples, and the DNeasy PowerWater Kit (Qiagen, Germany) for AT21 samples. While DNA extraction protocols can introduce technical variation in microbiome studies, previous work has shown that although extraction methods may affect DNA yield and sequencing efficiency, their influence on community composition or structure is generally weaker than environmental gradients (Rubin et al., 2014). To evaluate whether observed patterns were consistent with strong ecological structuring despite methodological differences, we performed pairwise PERMANOVA analysis among regions. All three regions differed significantly in community composition (Fram Strait vs. Kara Sea: $R^2 = 0.24$, $F = 18.5$, $p = 0.001$; Fram Strait vs. River Plume: $R^2 = 0.30$, $F = 19.6$, $p = 0.001$; Kara Sea vs. River Plume: $R^2 = 0.37$, $F = 19.1$, $p = 0.001$), indicating pronounced biogeographic separation between the three regions. Although sampling and extraction protocols differed between campaigns and cannot be fully disentangled from regional effects, the magnitude and consistency of community separation suggest that environmental gradients are the primary drivers. The V4 region of the 18S rRNA gene was amplified via polymerase chain reaction (PCR) using primers 528iF and 964iR (Fadeev et al., 2018). Metagenomic libraries were prepared following the Illumina 16S Metagenomic Sequencing Library Preparation protocol (Part # 15044223 Rev. B). The final library pool was prepared with 20% PhiX control (Thermo Fisher Scientific, USA), adjusted to a DNA concentration of 4 nM and

https://doi.org/10.5194/egusphere-2026-4192
Preprint. Discussion started: 17 July 2026

paired-end sequencing was conducted on a MiSeq platform (Illumina) across five separate runs. Demultiplexing and FASTQ sequence file generation were performed using the "Generate FASTQ" workflow of the MiSeq software. 18S rRNA sequences were processed using Cudadapt (v2.8; Martin, 2011) for primer and adapter removal, and the R package *dada2* (v1.18.0; Callahan et al., 2016) for sequence trimming and filtering, denoising with the Divisive Amplicon Denoising Algorithm (DADA), and paired-end merging. Runs were processed independently and merged prior to chimera removal and taxonomic assignment against the PR2 reference dataset (v4.14.0; Guillou et al., 2012) using the *dada2* implementation of the Naïve Bayesian Classifier (Wang et al., 2007).

Following taxonomic assignment, only amplicon sequencing variants (ASVs) assigned to one of six phytoplankton phyla (Chlorophyta, Cryptophyta, Dinoflagellata, Haptophyta, Ochrophyta, Prasinodermophyta) were retained. To improve taxonomic resolution, abundant ASVs lacking species-level classification were queried against the PR2 database and annotated with the percentage identity (pid) to their closest match. To account for contamination, blanks and PCR negative controls were sequenced alongside samples. ASVs were removed if their abundance in negative controls exceeded 10% of their abundance in corresponding samples (Wangensteen and Turon, 2016). Controls with < 400 total reads were excluded. Blank correction was performed using the R package *microDecon* (v1.0.2; McKnight et al., 2019). Only ASVs representing >0.005% of total reads across the entire dataset were kept for further analysis. Further details on the data processing are provided in Supplementary Table S2. The final dataset comprised 5096621 sequences from 72 samples comprising 479 ASVs affiliated with the phyla *Chlorophyta* (48), *Cryptophyta* (17), *Dinoflagellata* (252), *Haptophyta* (41), *Ochrophyta* (119) and *Prasinodermophyta* (2). Prior to calculating diversity indices, data were rarefied to the minimum sample size of 13521 reads using the *rrarefy* function from the vegan-package (v2.6.4; Oksanen et al., 2024) to standardize sequencing depth across samples.

2.5 Dissolved organic carbon, nitrogen and carbohydrates

Duplicate samples for dissolved organic carbon (DOC), total dissolved nitrogen (TDN), and high-molecular-weight (>1 kDa) dissolved combined carbohydrates (DCCHO) were collected in pre-combusted glass vials (500 °C for 8h). For DOC and TDN, 20 mL of seawater was filtered through a 0.45 µm GMF GD/X filter (Whatman, GE Healthcare Life Science, UK), acidified with 20 µL of hydrochloric acid (30% Suprapure, Sigma-Aldrich, Germany), and stored (+4°C). DOC and TDN were analysed simultaneously by applying the high-temperature catalytic oxidation method (TOC-VCSH, Shimadzu) following Engel and Galgani (2016) with a detection limit of 1 µmol L^{-1}. Seawater samples for DCCHO (20 mL) were filtered through 0.45 µm Acrodisk syringe filters (Pall Life Sciences, USA) and stored (-20 °C). After thawing, samples were desalted by membrane dialysis (1 kDa, Spectra Por) to exclude polysaccharides <1 kDa, oligosaccharides, and monosaccharides. Next, samples were hydrolysed with HCl (1 mol L^{-1}), neutralized by acid evaporation under a dinitrogen atmosphere and ultrapure water and analysed with high-performance anion exchange chromatography coupled with pulsed amperometric detection (HPAEC-PAD, DIONEX ICS3000DC) with a detection limit of 1 µg L^{-1}. A detailed description is given in Engel and Händel (2011). The analysis allows the quantification of neutral sugars (glucose, arabinose, fucose, galactose, rhamnose, mannose, and xylose),

https://doi.org/10.5194/egusphere-2026-4192
Preprint. Discussion started: 17 July 2026

amino sugars (galactosamine, glucosamine and muramic acid) and acidic sugars (galacturonic acid, glucuronic acid and gluconic acid). Mannose and xylose coeluted and were, therefore, quantified as a mixture. Muramic acid and gluconic acid were below the detection limit. Monomer concentrations and the individual numbers of carbon atoms were used to calculate the carbon concentration per litre, expressed as DCCHO-C and subsequently carbon-normalized sugar yields (%DOC) (eq. 1).

$$Yield\ (\%\ DOC) = [dCCHO - C]\ /\ DOC * 100 \quad (1)$$

Neutral sugar (NS) yields (%DOC; including fucose, rhamnose, arabinose, galactose, glucose, mannose and xylose) were used as an index of the relative contribution of freshly produced DOM and calculated according to equation 1.

Ratios of dissolved organic carbon (DOC) to dissolved organic nitrogen (DON) were calculated using measured DOC, total dissolved nitrogen (TDN) and inorganic nutrient (NO_3^- and NO_2^-) concentrations. DON was determined as the difference between TDN and the sum of inorganic nutrients.

2.6 Transparent exopolymer particles (TEP)

The gel-like particle species TEP was analysed according to Passow and Alldredge (1995) In brief, seawater samples were filtered in triplicates for spectrophotometric analysis. For each replicate 30-250 mL were filtered (<0.2 bar) onto 0.4 µm pore size polycarbonate filters (25 mm Nucleopore, track-etched, Whatman, GE Healthcare Life Sciences, UK), stained with 1 mL Alcian Blue Working Solution (0.02% final concentration, Alcian Blue 8GX, pH 2.5, Sigma Aldrich, Germany) for 5s and subsequently stored (-20°C). Prior to staining, the dye was stored at +4°C and filtered through 0.2 µm syringe filters (Acrodisk, Sigma Aldrich) right before use. Blanks were prepared from 10 mL of distilled water and processed like the samples. In preparation for the spectrophotometric analysis, each filter was covered in 6 mL of sulfuric acid (H_2SO_4, 80%) and incubated for 2 hours. The absorbance of Alcian Blue was measured at 787 nm in a 1 cm cuvette against distilled water. Finally, concentrations are given in micrograms of Xanthan equivalents per litre (µg Xeq. L^{-1}) and calculated using the following equation:

$$TEP\ (\mu g\ Xeq.L^{-1}) = \frac{(E_{787} - C_{787})}{V} \times F(x) \quad (2)$$

with E_{787} being the absorption of the sample, C_{787} the absorption of the blank, V the filtered volume in L and F the determined calibration factor for the standard polysaccharide Gum Xanthan.

2.7 Statistical analysis

All figures were generated using the ggplot2 package (v3.5.2; Wickham, 2016) and all statistical analyses and calculations were conducted using R (v4.3.3) and the R Studio interface (v2023.12.1). Differences in chl-*a* and DOM concentration among water masses and regions were assed using the *kruskal.test* function for Kruskal-Wallis rank sum tests (*stats* package) and mean chl-*a* concentrations were evaluated via Fisher-Pitman permutation test (*oneway_test, coin* package, v1.4.3; Hothorn et al., 2006). Principal Component Analysis (PCA) was performed on standardized DCCHO data (mol%) using the *rda*-function in the *vegan* package (v2.6.4; Oksanen et al., 2024) to identify patterns in carbohydrate composition across regions.

https://doi.org/10.5194/egusphere-2026-4192
Preprint. Discussion started: 17 July 2026

Community analyses of the 18S amplicon data were based on Hellinger-transformed relative abundances of ASVs using Bray-Curtis dissimilarity distances and included non-metric multidimensional scaling (NMDS), permutational multivariate analysis of variance (PERMANOVA), hierarchical clustering and an indicator species analysis. NMDS and a PERMANOVA with 999 permutations were performed to test for differences in protist community composition between geographical regions and water layers, using the functions *metaMDS* and *adonis* from the *vegan* package (v2.6.4; Oksanen et al., 2024). Then, hierarchical clustering was applied to assess community patterns within regions previously identified by applying the *hclust* function set to average linkage (*stats* package). The reliability of the clusters and the optimal number of groups were evaluated with silhouette widths using *silhouette* from the *cluster* package (v2.1.6; Maechler et al., 2023). Furthermore, an indicator species analysis was performed on relative abundance data to detect ASVs significantly associated with the three identified. The analysis was conducted using the *multipatt* function of the *indicspecies* package (version 1.8.0; De Cáceres & Legendre, 2009), applying the r.g option (point biserial correlation coefficient) and 9999 permutations to assess statistical significance. The indicator statistic value (stat) represents the strength of association between ASVs and habitats, with values close to 1 indicating a perfect association. In doing so, the *stat* value accounts for both the occurrence of an ASV in a given group (presence/absence) and its relative abundance across all samples. As a result, ASVs that occur exclusively in one group, even at low abundances, as well as ASVs that are present in more than one group but are more abundant in a specific group, can yield high association values. The top 30 ASVs with the highest stat values and $p < 0.01$ were then selected for further analysis and correlated with DCCHO (mol%). Correlations were calculated using Spearman's rank correlation coefficient with *cor* and *cor.test* functions in *stats* package (v4.3.3). To further evaluate the relationship between protist community composition and DCCHO, a Mantel test with 999 permutations and Spearman's rank correlation was performed using the *mantel* function (*vegan* v2.6.4), comparing Bray-Curtis distances of Hellinger-transformed ASVs with Euclidean distances of standardized mol% DCCHO. The redundancy analysis (RDA) was conducted using *rda* function form the *vegan* package to assess the abiotic drivers of protist community composition. Prior a detrended correspondence analysis (*decorana*, vegan) was performed to confirm the use of linear methods. Collinearity was checked via variance inflation factors (>10 excluded, *vif.cca*, vegan) and forward selection (999 permutations, *ordiR2step*, vegan) identified key environmental predictors. The significance of the overall model, individual axes and each term was tested using permutation tests (999 permutations, *anova.cca*, vegan). Significance of environmental vectors was assessed using permutation tests of vector-ordination correlations using *envfit* function (999 permutations) in the vegan package.

3. Results

3.1 Hydrographic conditions and inorganic nutrients

Four different water masses were identified based on potential temperature and absolute salinity, following Rudels et al. (2000) and Meyer et al. (2017): Atlantic Water (AW), Mixed Atlantic Water (MAW), Polar Surface Water (PSW) and warm Polar Surface Water (wPSW) (Fig. S3). All four water masses occurred in the Fram Strait (FS), whereas AW was absent from both

https://doi.org/10.5194/egusphere-2026-4192
Preprint. Discussion started: 17 July 2026

the Kara Sea (KS) and the Ob-Yenisei River Plume (RP) (Table 1). The FS was characterized by a pronounced east-west gradient, with warm (2.9 ± 0.2°C), saline (34.9 ± 0.1) AW occurring in the east and colder (-1.1 ± 0.3°C), less saline (33.4 ± 0.7) PSW in the west, while wPSW and MAW prevailed in the transition zone. The observed spatial distribution is consistent with established EGC and WSC flow patterns. In the KS, MAW and wPSW were primarily associated with the western Kara Sea along the St. Anna Trough. The wPSW generally dominated the surface layer, while the more saline MAW (34.6 ± 0.1) was exclusively detected in the SCM layer. In contrast, colder (-1.1 ± 0.6) and fresher (33.2 ± 0.9) PSW was found along the northern shelf edge. Vertical salinity differences between the surface and the SCM were slightly more pronounced in the KS (surface 33.3 ± 0.8; SCM: 34.2 ± 0.4) than in the FS (surface: 33.8 ± 0.9; SCM: 34.2 ± 0.8). In the RP, only wPSW was observed, with a single exception. This water mass was markedly warmer (4.3 ± 1.5) and substantially less saline (15.5 ± 5.5) than wPSW in either FS or KS.

Nutrient concentrations varied by water mass and region (Table 1). In wPSW, nitrate decreased sharply from 3.4 ± 2 µmol L^{-1} in the FS to 1.4 ± 3 µmol L^{-1} in KS, reaching a minimum in the RP (0.2 ± 0.6 µmol L^{-1}). Highest nitrate and phosphate concentrations were generally observed in AW and MAW, with nitrate reaching ~7 µmol L^{-1} in the FS and ~3 µmol L^{-1} in the KS, while phosphate ranged from 0.4 to 0.7 µmol L^{-1}. Regional contrasts were pronounced, with nitrate, phosphate and silicate concentrations more than twice as high in the FS than in the KS, whereas nitrite concentrations were approx. fivefold higher in the KS. In the RP, concentrations of most nutrients were near or below the detection limit, except for silicate, which remained high, reaching 34.5 ± 13.7 µmol L^{-1} in wPSW and 39.2 µmol L^{-1} in PSW.

Table 2: Arithmetic mean ± standard deviation of temperature, salinity and inorganic nutrient concentrations for four water masses Atlantic Water (AW), Modified Atlantic Water (MAW), warm Polar Surface Water (wPSW) and Polar Surface Water (PSW) sampled in the Fram Strait (FS; n = 38), Kara Sea (KS; n = 24) and Ob-Yenisei River Plume (RP; n = 11). Water masses were defined following Rudels et al. (2000) and Meyer et al. (2017).

Region	Water mass	Temperature [°C]	Salinity	NO_3^- [µmol L^{-1}]	NO_2^- [µmol L^{-1}]	PO_4^{3-} [µmol L^{-1}]	$Si(OH)_4$ [µmol L^{-1}]
Fram Strait	**AW** (n=7)	2.93 ± 0.2	34.9 ± 0.1	7.11 ± 1.1	0.1 ± 0.01	0.5 ± 0.1	1.8 ± 0.6
	MAW (n=1)	0.7	34.6	7.8	0.02	0.7	3.1
	wPSW (n=11)	2.5 ± 1.4	34.5 ± 0.5	3.4 ± 2	0.1 ± 0.03	0.3 ± 0.1	1.4 ± 0.5
	PSW (n=19)	-1.1 ± 0.3	33.4 ± 0.7	1.6 ± 1.6	0 ± 0.01	0.3 ± 0.1	1.5 ± 1.3
Kara Sea	**MAW** (n=4)	-0.1 ± 0.7	34.6 ± 0.1	3.1 ± 2.2	0.3 ± 0.2	0.4 ± 0.3	1.1 ± 0.8
	wPSW (n=11)	1.6 ± 1	33.9 ± 0.4	1.4 ± 3	0.1 ± 0.1	0.2 ± 0.2	0.8 ± 1.5

https://doi.org/10.5194/egusphere-2026-4192
Preprint. Discussion started: 17 July 2026

	PSW (n=9)	-1.1 ± 0.6	33.2 ± 0.9	1.6 ± 1.9	0.09 ± 0.09	0.1 ± 0.08	0.4 ± 0.5
River Plume (OY)	**wPSW** (n=10)	4.3 ± 1.5	15.5 ± 5.5	0.2 ± 0.6	0.07 ± 0.03	0.14 ± 0.07	34.5 ± 13.7
	PSW (n=1)	-0.55	23	0.1	0.1	0.1	39.2

3.2 Chlorophyll-a distribution

While the depth of the SCM layer was on average 18 m in the FS and 31 m in the KS (Fig. S1), chl-*a* concentration did not differ significantly between regions (Fisher-Pitman, p = 0.85) or among water masses (Kruskal-Wallis, p = 0.08). Generally, chl-*a* appeared to be highly patchy across the sectors with less pronounced vertical differences in the FS (surface: 2.1 ± 1.1 µg L^{-1}; SCM: 2.2 ± 1.1 µg L^{-1}), yet the highest (SCM: 3.3 ± 2.9 µg L^{-1}) and lowest concentrations (surface: 1.1 ± 2.2 µg L^{-1}) across water layers in the KS (Fig. 2). Although no underway measurements were available, data from CTD station 113 in the RP showed values comparable to the KS surface layer (1.1 µg L^{-1}). At the regional scale, differences between selected water masses emerged. In the KS, chl-*a* was fourfold lower in the wPSW (0.8 ± 1.2 µg L^{-1}) than in the PSW (4.1 ± 3.4 µg L^{-1}; Table S3). In the FS, differences were less pronounced, ranging from 1.2 µg L^{-1} in AW to 2.6 µg L^{-1} in wPSW. Notably, exceptionally high concentrations were measured at the SCM of stations 41 and 47 and at both the surface and SCM of station 61 (7-8 µg L^{-1}; n = 4).

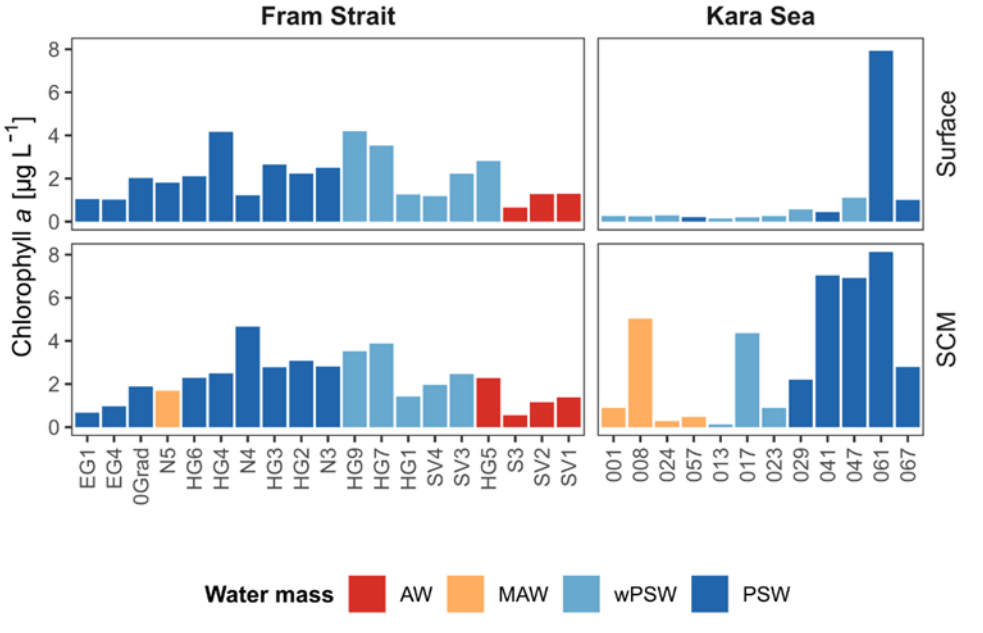

https://doi.org/10.5194/egusphere-2026-4192
Preprint. Discussion started: 17 July 2026

Figure 2: Chlorophyll *a* concentration (µg L^{-1}) at the surface and subsurface chlorophyll *a* maximum (SCM) layer at each station. Colours indicate water mass: AW (Atlantic Water), MAW (Modified Atlantic Water), PSW (Polar Surface Water), wPSW (warm Polar Surface Water).

3.3 Spatial distribution of dissolved biopolymers and transparent exopolymer particles (TEP)

Clear regional patterns emerged with the highest DOC and DCCHO concentrations in the RP, whereas TEP concentrations peaked in the FS (Fig. 3A). DOC varied significantly among regions (Kruskal–Wallis: $\chi^2 = 32.17$, df = 2, $p < 0.001$), peaking in the RP (335 ± 94 µmol L^{-1}) and being consistently higher in the FS (surface: 81 ± 13; SCM: 79 ± 16 µmol L^{-1}) than in the KS (surface: 75 ± 11; SCM: 69 ± 9 µmol L^{-1}). DCCHO showed a similar regional trend (Kruskal–Wallis: $\chi^2 = 30.03$, df = 2, $p < 0.001$), with the highest values in the RP (2609 ± 862 nmol L^{-1}), roughly twofold higher than in the FS (surface: 1250 ± 576 nmol L^{-1}; SCM: 990 ± 376 nmol L^{-1}) and about fourfold higher in the KS (surface: 735 ± 154; SCM: 786 ± 426 nmol L^{-1}). In contrast, TEP concentrations were highest in the FS (surface: 226 ± 115; SCM: 219 ± 210 µg Xeq L^{-1}, n=19), approximately fourfold greater than in the KS (surface: 41 ± 22; SCM: 47 ± 32 µg Xeq L^{-1}, n=12) or the RP (59 µg Xeq L^{-1}, n=1), with significant differences among regions (Kruskal–Wallis, $\chi^2 = 24.80$, df = 2, $p < 0.001$). Differences among water masses were generally less pronounced, but DOC, DCCHO and TEP concentrations were highest in PSW compared with AW and MAW (Table S3), with TEP reaching maxima at the northern stations (surface: 472 ± 31 µg Xeq L^{-1} at N3; SCM: 949 ± 143 µg Xeq L^{-1} at N4; Fig. S4). Although DCCHO concentrations in the FS were less than twofold higher than in the KS, TEP concentrations were more than fourfold higher, leading to markedly higher TEP:DCCHO ratios in the FS, particularly in the PSW and wPSW in the SCM (FS: ~0.7; KS: ~0.2; Fig. S5).

Furthermore, we observed regional differences in DOM quality and origin (Fig. 3A). Neutral sugar yields (NS %DOC) were highest in the FS (surface: 9 ± 5%; SCM: 7 ± 3%), followed by the KS (surface: 5 ± 1%; SCM: 6 ± 3%) and RP (4 ± 1%). In contrast, DOC:DON ratios peaked in the RP (29 ± 4), while FS (surface: 11 ± 3; SCM: 9 ± 5) and the KS (surface: 12 ± 3; SCM: 8 ± 3) ratios were similar, with greater vertical variability in the KS. Together, these proxies indicate terrestrial influence in the RP and surface KS layers and fresher material in the FS.

Compositional analysis of DCCHO (mol%) using principal component analysis (PCA) revealed that PC1 (33.4% variance explained) separated RP and FS, whereas PC2 (29.2%) distinguished RP and KS samples (Fig. 3B). Glucose and mannose + xylose dominated across all regions (FS: 34-42 and 29-35 mol%; KS: 34-36 and 33-42 mol%; RP 24 and 29 mol%, respectively) (Fig. 3C). Rhamnose and arabinose were enriched in FS (surface: 4.8 mol% and 8.7 mol%; SCM: 5.3 mol% and 8.1 mol%, respectively), while galactose and fucose were highest in RP (14.2 mol% and 9.6 mol% respectively). KS samples contained on average a higher proportion of amino sugars (galactosamine: 0.8-0.9 mol%; glucosamine: 5-6.4 mol%).

https://doi.org/10.5194/egusphere-2026-4192
Preprint. Discussion started: 17 July 2026

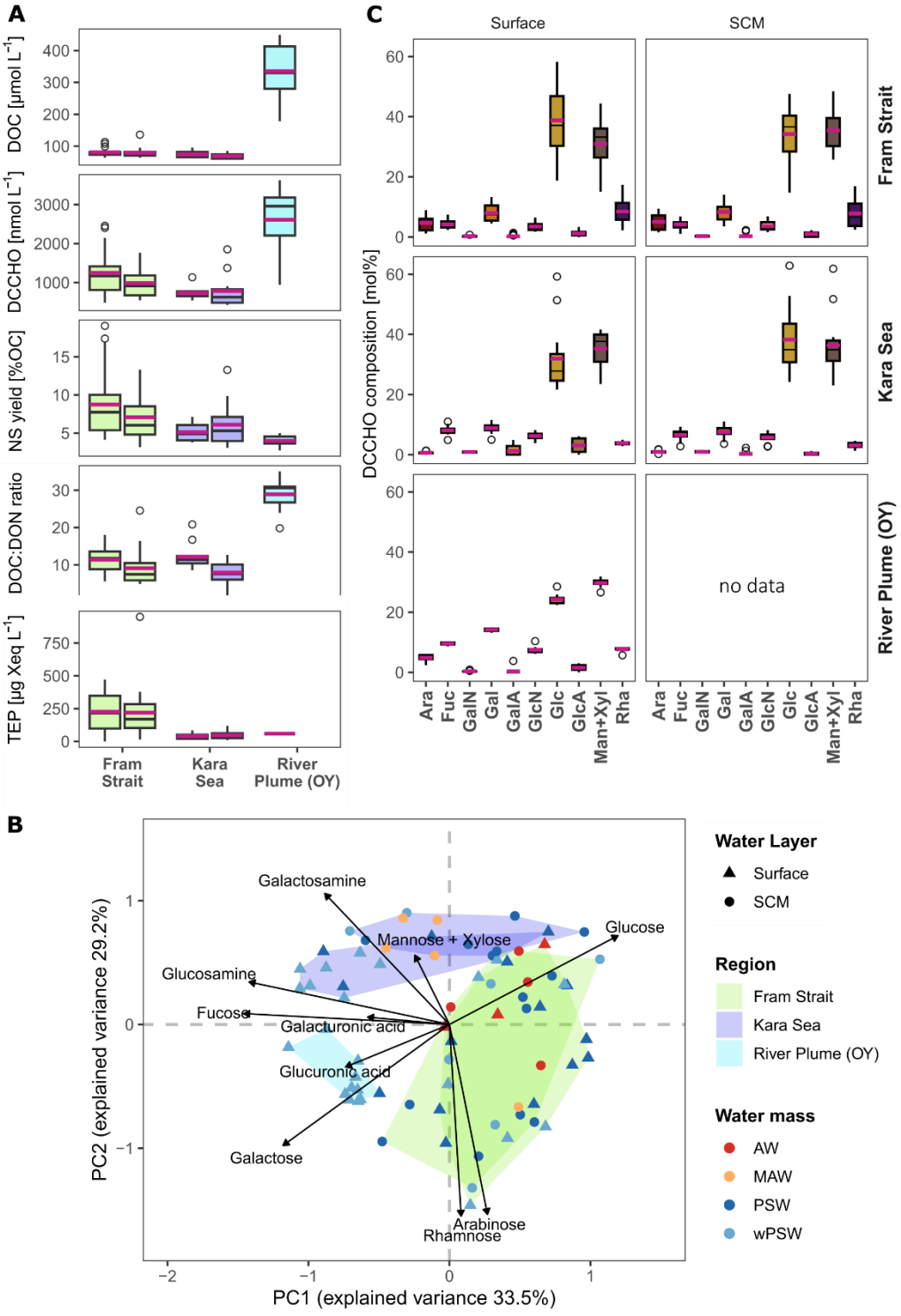

Figure 3: Characteristics of dissolved organic matter (DOM) properties across three Arctic regions at the surface and in the subsurface chlorophyll *a* maximum (SCM) layer. (A) Boxplots of DOM characteristic top to bottom: dissolved organic carbon (DOC)

https://doi.org/10.5194/egusphere-2026-4192
Preprint. Discussion started: 17 July 2026

in µmol L^{-1}, dissolved combined carbohydrates (DCCHO) in nmol L^{-1}, neutral sugar yields (NS yields %DOC) of DOC, DOC:DON ratios and transparent exopolymer particles (TEP) expressed in µg Gum Xanthan L^{-1} equivalents for each water layer. The horizontal black line indicates the median, the magenta line the mean, the box shows the interquartile range, and whiskers extend to 1.5× the interquartile range. Colours represent geographical regions. (B) Principal component analysis (PCA) based on DCCHO composition (mol%). Colours indicate geographical region, and shape indicates water layer, and point colour denotes water mass: AW (Atlantic Water), MAW (Modified Atlantic Water), PSW (Polar Surface Water), wPSW (warm Polar Surface Water). Arrow length illustrates the strength of the contribution of individual sugars in driving sample distribution. (C) Composition of DCCHO (mol%) grouped by water layer and region. Abbreviations: Ara, arabinose; Fuc, fucose; GalN, galactosamine; Gal, galactose; GalA, galacturonic acid; GlcN, glucosamine; Glc, glucose; GlcA, glucuronic acid; Man+ Xyl, mannose + xylose; Rha, rhamnose.

The composition of DCCHO also varied within regions and across bloom conditions (Fig. 4, Table S4). Bloom conditions were defined as both chl-*a* concentrations > 1 µg L^{-1} and NS yields > 5.9 %DOC, with the latter threshold indicating fresh DOM (Amon & Benner, 2003). Samples not meeting the criteria were classified as non-bloom samples. In both the FS and KS, bloom samples showed a twofold increase in DCCHO concentrations compared to non-bloom samples. However, this increase was accompanied by region-specific changes in the relative contributions of individual carbohydrates (Table S4).

In the FS, several carbohydrates contributed more strongly under bloom conditions, including arabinose, which increased from 4% to 5.5%, rhamnose from 7% to 9%, and glucose from 34.3% to 38.3%, alongside a twofold increase in acidic sugars. To assess whether these shifts represented enrichment trends, bloom-to-non-bloom molar ratios were calculated and tested against 1 using Wald tests on log-transformed ratios, with standard errors estimated by Gaussian error propagation. Ratios exceeded 1 for rhamnose, arabinose, glucose, galacturonic acid, and glucuronic acid, indicating a broader enrichment trend across neutral and acidic sugars (Fig. 4). Although most enrichments were not statistically significant across the full FS bloom dataset, restricting the analysis to samples with particularly high NS yields (>10 %DOC, above the upper limit of 9.6 reported by Amon and Benner (2003)) revealed significant enrichments in arabinose, glucose, and glucuronic acid, together with significant decreases in fucose and amino sugars (Table S4). In contrast, the compositional shift in the KS was mainly limited to glucose, which increased from 32.3% to 49.3%, while the relative contributions of most other carbohydrates decreased under bloom conditions. Accordingly, glucose was the only carbohydrate with a significant bloom-to-non-bloom molar ratio above 1 (1.5), whereas most other compounds showed ratios below 1. Significant declines occurred in fucose, rhamnose, arabinose, galactose, glucuronic acid, and the amino sugars, while mannose + xylose showed no significant change.

https://doi.org/10.5194/egusphere-2026-4192
Preprint. Discussion started: 17 July 2026

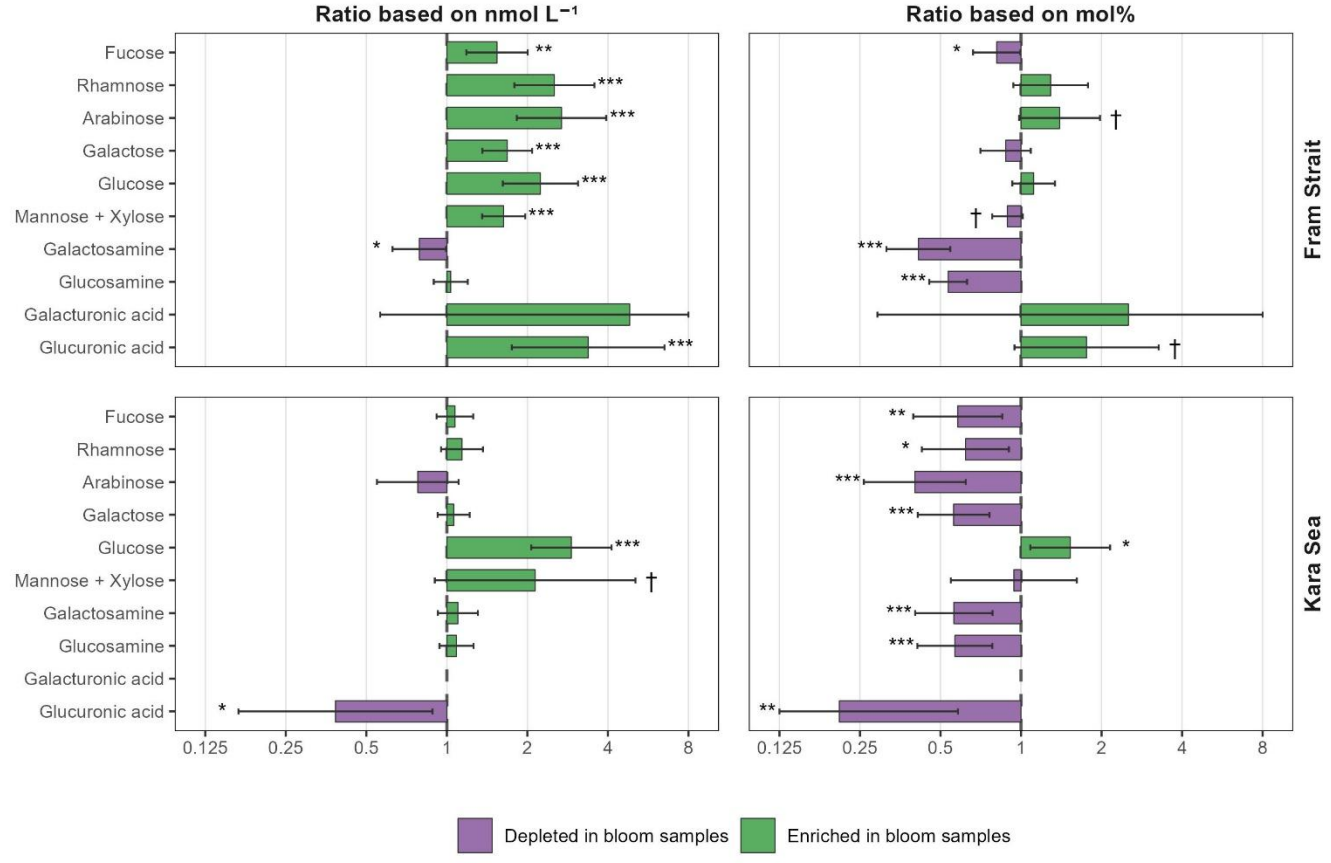

Figure 4: Bloom vs. no-bloom ratios of dissolved combined carbohydrate concentrations and molar percentages in Kara Sea and Fram Strait. Ratios are plotted on a log_2-transformed axis for symmetry, while x-axis labels show the corresponding untransformed ratio values. Green bars indicate enrichment in bloom samples and purple bars indicate depletion. Error bars show 95% confidence intervals and symbols denote p-value thresholds: † p < 0.10, * p < 0.05, ** p < 0.01, and *** p < 0.001.

3.4 Protist community composition

3.4.1 Differences among geographical regions

Protist communities grouped into three significantly distinct clusters corresponding to the FS, KS and RP (PERMANOVA, $R^2 = 0.33$, $F = 16.79$, $p = 0.001$; Fig. 5A). The FS represented the largest cluster (38 samples, 390 ASVs), followed by the KS (23 samples, 375 ASVs) and RP (11 samples, 315 ASVs; Fig. S2). The FS assemblage showed the highest ASV richness, particularly within the SCM (200), yet low evenness resulted in a low overall Shannon diversity (surface: 2.8; SCM: 2.7) (Fig. S6). Conversely, the RP and the KS surface layer exhibited the highest Shannon diversity (3.2 and 3.3, respectively) driven by high evenness (0.66 and 0.62) but low richness (158 and 169), whereas the SCM in the KS was characterised by low richness (142) but highly variable evenness and diversity.

https://doi.org/10.5194/egusphere-2026-4192
Preprint. Discussion started: 17 July 2026

Community composition differed among regions, even at the phylum level (Fig. 5B, Table S5). In the FS, dinoflagellates (43% in the surface) and haptophytes (39% in the SCM) dominated the community, with *Phaeocystis pouchetii* (~89%) as the most prevalent haptophyte ASV (Table S6). Ochrophytes 18% surface and 20% SCM), the third largest group, were dominated by the diatom *Chaetoceros gelidus* (48% and 71%). Across depth layers, no significant differences in community composition were observed (PERMANOVA, $R^2 = 0.028$, $F = 1.02$, $p = 0.41$).

In the KS, haptophytes accounted for only a small proportion of the community (4% surface and 2% SCM), and overall community composition differed significantly with depth (PERMANOVA, $R^2 = 0.107$, $F = 2.51$, $p = 0.007$). Dinoflagellates prevailed at the surface (56%), while Ochrophyta dominated the SCM (52%). Among Ochrophyta, the diatom *Thalassiosira rotula* dominated the surface (19%), while an ASV matching *Eucampia groenlandica* (100% pid) prevailed in the SCM (46%), followed by *T. rotula* (11%). Among dinoflagellates *Gyrodinium helveticum* (20%) and *Karlodinium veneficum* (14%) were most abundant.

As in the KS, dinoflagellates strongly dominated the RP cluster (57%), followed by ochrophytes (25%), while cryptophytes reached up to fivefold higher abundances (8%) than in the other regions. The most abundant ASVs were an unknown dinophyte (35%; highest similarity to *Karenia papilionacea* (pid 99.7) and *Prorocentrum* sp. (pid 99.7), the diatom *Chaetoceros neogracilis* (32%), and the cryptophyte *Teleaulax gracil*s (64%). Interestingly, chlorophytes varied only slightly among regions (4–8%), but were dominated by *Micromonas polaris*, whose relative abundance within Chlorophyta ranged from 29% in the RP to 94% in the KS surface. Within the Ochrophyta, diatoms (*Bacillariophyceae*) were most abundant in all clusters (77-94%), yet slightly declined as golden algae (*Chrysophyceae*) increased to 15% in the RP and 13% in the surface KS, with ASVs belonging to the genus *Dinobryon* being the most abundant (38-94%; Table S7).

https://doi.org/10.5194/egusphere-2026-4192
Preprint. Discussion started: 17 July 2026

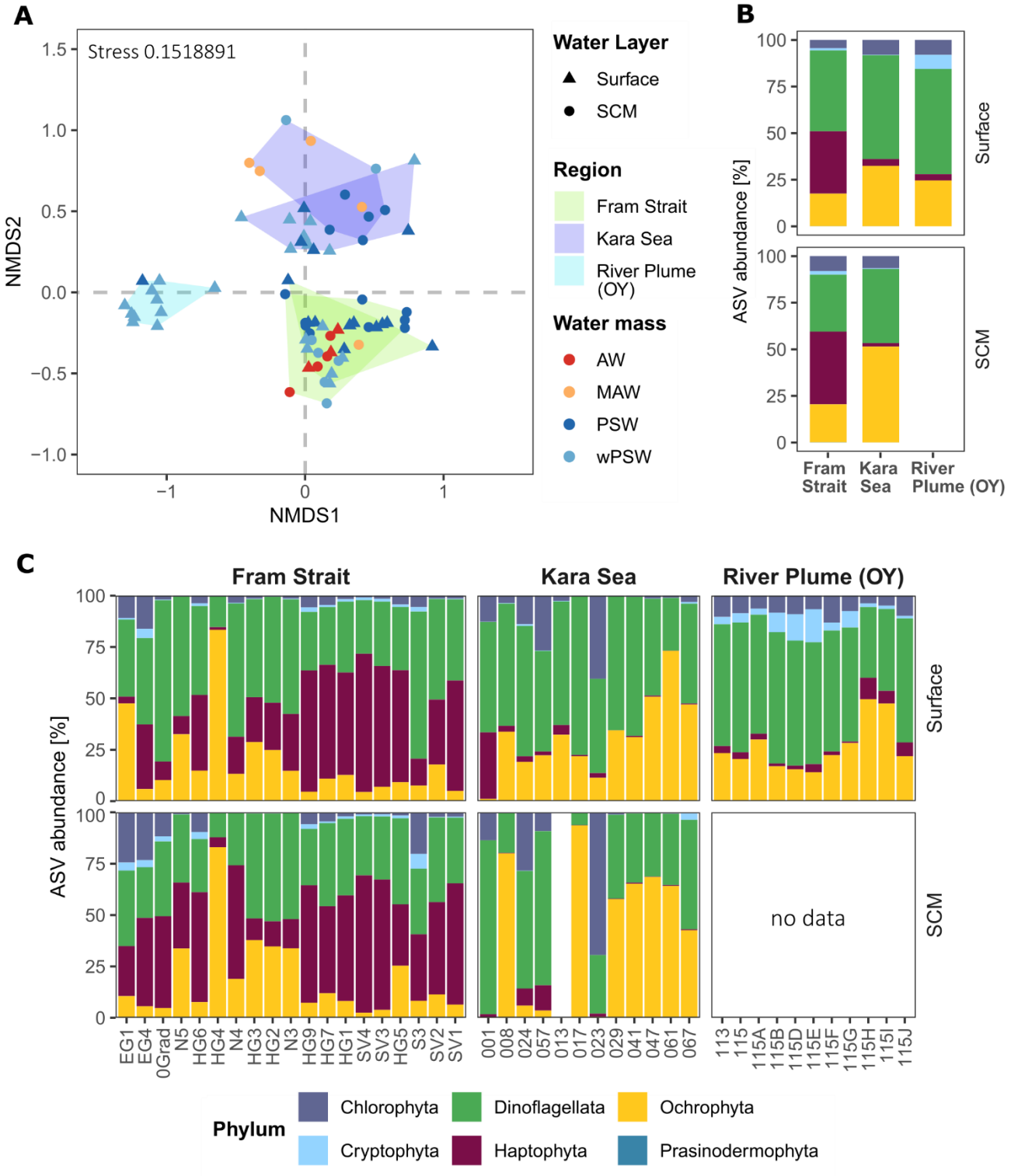

Figure 5: Spatial distribution patterns of phytoplankton community composition at the surface and in the subsurface chlorophyll *a*

https://doi.org/10.5194/egusphere-2026-4192
Preprint. Discussion started: 17 July 2026

maximum layer (SCM): (A) Non-metric multidimensional scaling (NMDS) plot illustrating differences in protist community composition between regions. The ordination is based on Bray-Curtis dissimilarity distances of Hellinger-transformed amplicon sequence variants (ASVs). Colours indicate geographical region, shape indicates water layer, and point colour denotes water mass: AW (Atlantic Water), MAW (Modified Atlantic Water), PSW (Polar Surface Water), wPSW (warm Polar Surface Water). The 2D stress value is displayed in the plot. (B) Mean relative abundance of ASVs grouped by phytoplankton phylum level for each region. (C) Relative abundance of phytoplankton ASVs grouped at the phylum level across individual samples. Colours represent phytoplankton phyla.

3.4.2 Variability within geographical regions

While protist community composition differed strongly among regions, notable within-region variability was also observed (Fig. 5C). Hierarchical clustering identified two to four robust clusters per region (Fig. S7). Although cluster numbers were similar between depth, station assignment differed, particularly in the KS.

In the FS, two clusters were observed across depth. One cluster was dominated almost entirely by a single ASV assigned to *Chaetoceros gelidus*, accounting for 72% at the surface and 79% at SCM of HG4, with lower contributions at nearby stations (25% SCM HG3 and 21% SCM HG2). The second cluster was characterized by low ochrophyte contributions and instead a dominance of *Phaeocystis pouchetii*, (~32% surface; ~40% SCM).

In the KS, clustering differed strongly between surface and SCM samples. In surface waters, two of the three clusters corresponded to station 61, dominated by ochrophytes (73%), with the two most abundant ASVs assigned to the genus *Thalassiosira* (38%), and station 29, dominated by the dinoflagellate *Gyrodinium helveticum* (44%). The remaining stations formed the third cluster defined by *Gyrodinium* spp. and the chlorophyte *Micromonas* sp. In the SCM, the largest cluster (stations: 8, 17, 41, 29, 47, 61, 67) was characterised by diatoms, primarily *Thalassiosira* spp. and *Eucampia* spp. Stations 8 and 17 were dominated by *Eucampia* sp. (77–88%), stations 29, 41 and 47 exhibited mixed assemblages, while stations 61 and 67 had higher *Thalassiosira* spp. contributions (45% and 16%). The second SCM cluster (stations: 24, 57) was characterised by *Micromonas polaris* (~19%), followed by *Karlodinium* sp. (~9%), while in the third cluster (stations: 1, 23) an unknown Dinophyceae lineage (~39%) and *M. polaris* (~34%) prevailed.

Four subclusters were identified in the RP. The first (stations: 113, 115, 115A) and second (stations: 115B-G) cluster were dominated by *Gymnodinium* sp. (16% and 11%) and unidentified dinoflagellates (single ASVs between 16 and 26%), with Cluster 2 showing higher cryptophyte contributions, particularly *Teleaulax gracilis* (7%). A third cluster (stations: 115H, 115I) was defined by the diatom *Chaetoceros neogracilis* (22%), whereas a fourth cluster (115J) was characterised by a *Gymnodinium* sp. ASV (15%) distinct from those in the other clusters, and notable contributions of dinoflagellates *Biecheleria* sp. (10%) and *Gyrodinium spirale* (9%).

3.4.3 Region-specific protist indicator species

To identify individual taxa with a high prevalence for a specific geographical region, we conducted an indicator species analysis. In total, 236 ASVs were identified as significant indicators ($p \leq 0.01$ & stat ≥ 0.3) for FS (68), KS (52), and the RP (116). Identified indicator taxa were distinct among regions, but not restricted to them (Fig. 6 and Table S8). We focused on

https://doi.org/10.5194/egusphere-2026-4192
Preprint. Discussion started: 17 July 2026

abundant indicator taxa, as we expect them to exert a stronger influence on biogeochemical processes. For the FS, *Phaeocystis pouchetii* (p=0.0001, stat=0.8) was most abundant ~32.4%, even reaching ≥50% (stations: SV1, SV3, SV4, HG9), followed by *Heterocapsa* sp. with ~1.7% and up to 11% at station N3. In the KS, the most abundant ASV was assigned to the diatom genus *Eucampia* (p=0.0006, stat=0.43), with an average of 15.4% and a wide range from less than 1% to 63% across stations, along with the dinoflagellate *Karlodinium* sp. (~3.4%). The RP was characterised by dinoflagellate indicator species, the most abundant ASV (p=0.0001, stat=0.82, averaging 19.1%) being an unidentifiable dinoflagellate showing 99.7% similarity the genera *Gyrodinium* and *Prorocentrum*.

https://doi.org/10.5194/egusphere-2026-4192
Preprint. Discussion started: 17 July 2026

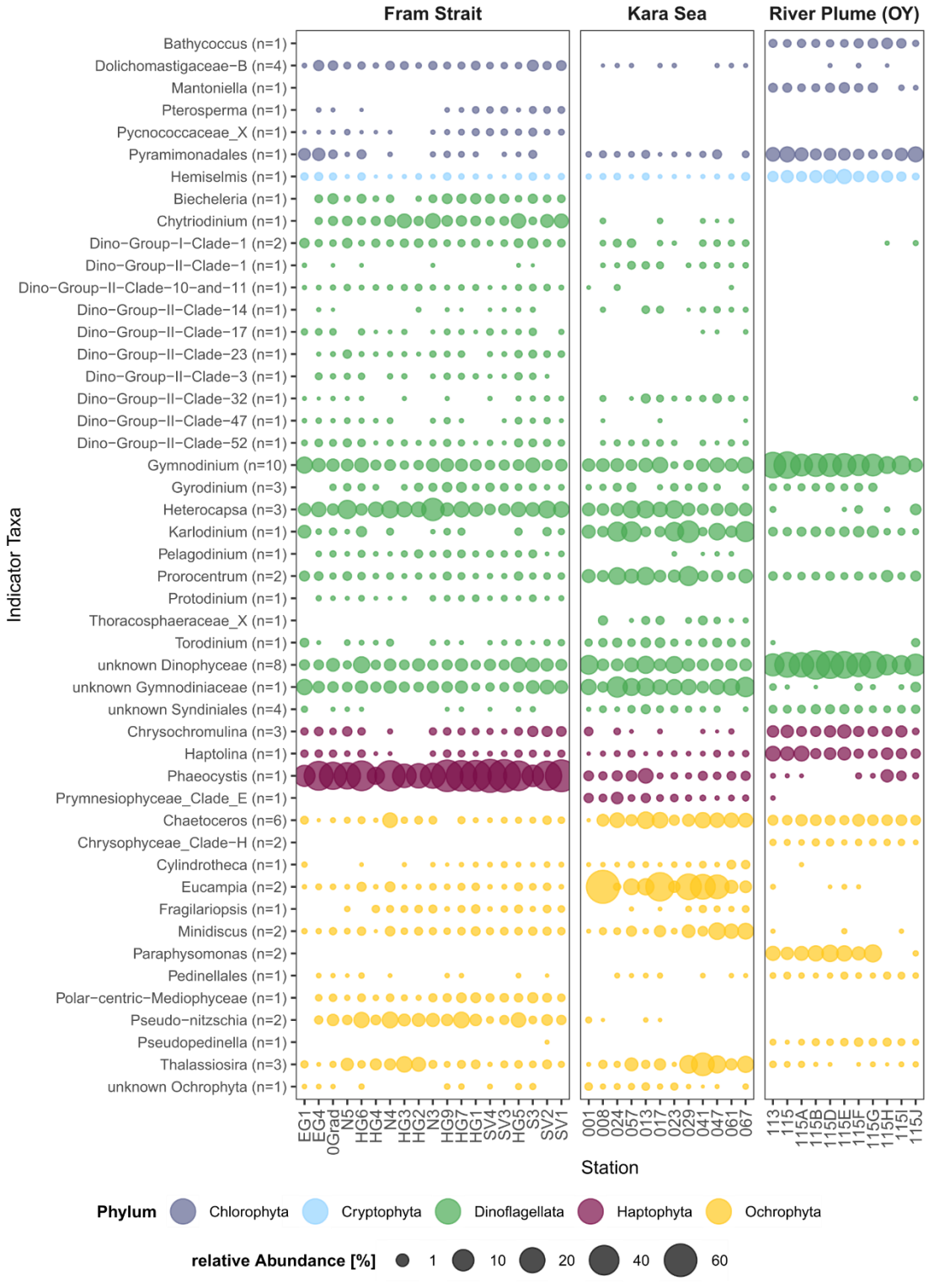

Figure 6: Bubble chart of protist indicator taxa abundance across stations, grouped by region. The 30 ASVs with the highest stat

https://doi.org/10.5194/egusphere-2026-4192
Preprint. Discussion started: 17 July 2026

values per region were grouped at the genus level whenever possible, with n denoting the number of ASVs contributing to a given taxon. Where genus-level assignment was not feasible, higher taxonomic groups were used. Bubble sizes are proportional to the square root of relative abundance (%) and coloured by phylum. Note that indicator taxa identified for a particular region are not restricted to that region and are also present in other regions (Table. S7).

3.5 Environmental drivers of community composition

The RDA model explained approximately 23% of protist community variation (Fig. 7A). Forward selection identified salinity, nitrite (NO_2^-) and phosphate (PO_4^{-3}) as significant predictors, whereas temperature showed only a weak effect and silicate (SiO_2) as well as nitrate (NO_3^-) were excluded due to multicollinearity. Permutation tests confirmed that the overall model was significant ($F = 5.04$, $p = 0.001$) and that salinity ($F = 10.57$, $p = 0.001$), NO_2^- ($F = 4.09$, $p = 0.001$) and PO_4^{-3} ($F = 3.66$, $p = 0.001$) contributed significantly, whereas temperature was not significant at $\alpha = 0.05$ ($F = 1.82$, $p = 0.068$). Only the first two canonical axes were significant (RDA1: $F = 11.85$, $p = 0.001$; RDA2: $F = 5.89$, $p = 0.001$) and retained for interpretation. Assemblages from the KS were primarily associated with elevated NO_2^-, whereas FS communities were more strongly related to PO_4^{-3}. RP assemblages aligned with lower salinity, higher temperatures, and higher $Si(OH)_4$ concentrations.

https://doi.org/10.5194/egusphere-2026-4192
Preprint. Discussion started: 17 July 2026

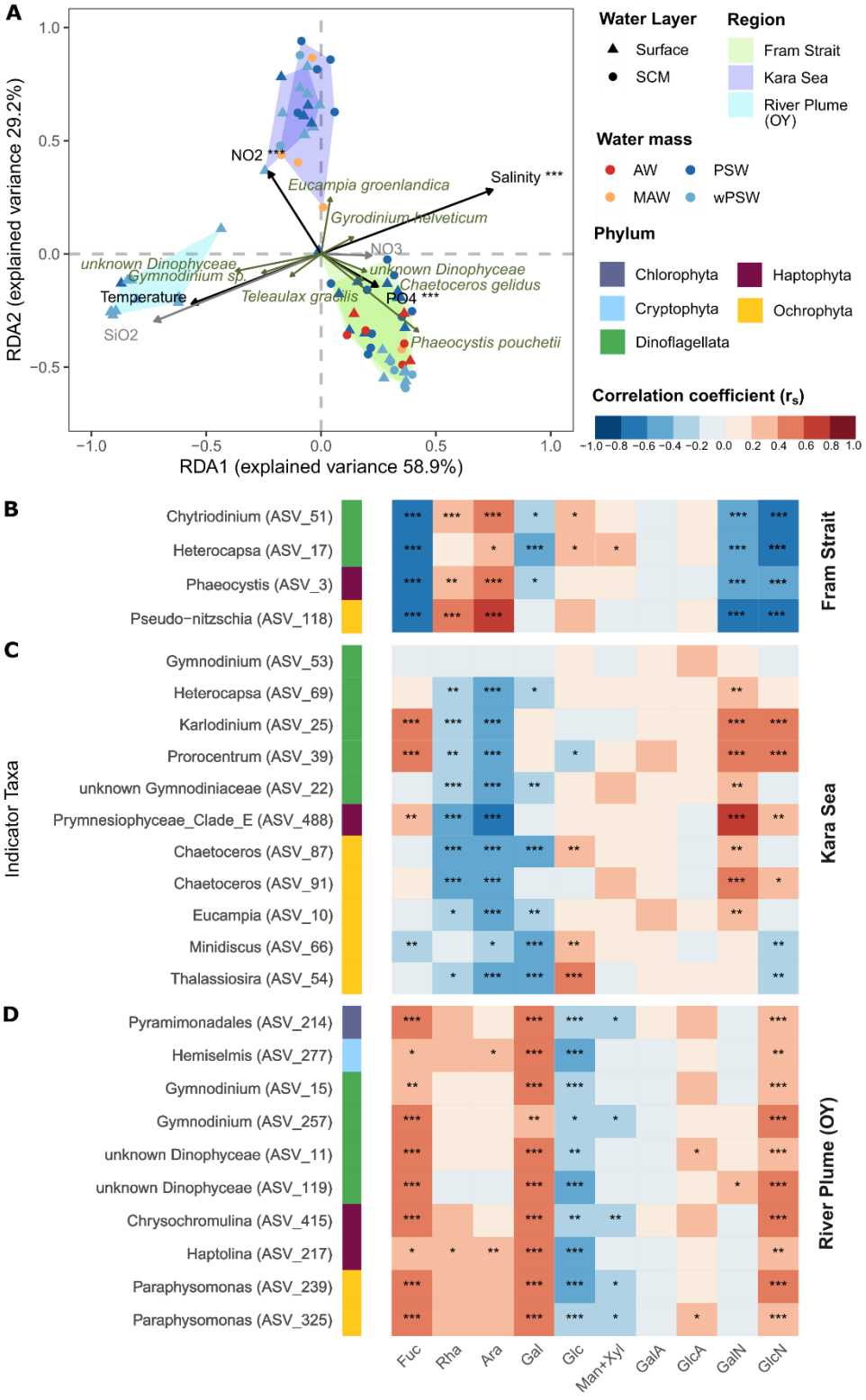

Figure 7: Redundancy Analysis (RDA) of phytoplankton community composition and environmental drivers (A). Convex hulls show

https://doi.org/10.5194/egusphere-2026-4192
Preprint. Discussion started: 17 July 2026

geographical regions, point colours indicate water masses and shapes denote water layers. Arrows represent environmental variables identified via forward selection (black = selected, gray = excluded), with significance assessed by permutation tests of RDA model terms (999 permutations). Green arrows indicate the 8 most abundant ASVs across all samples, highlighting taxa contributing most strongly to community variation. Panels B - D illustrate pairwise Spearman correlations of relative abundances of phytoplankton indicator ASVs (relative abundances >1%) with dissolved carbohydrates (DCCHO, mol%) for Fram Strait (B), Kara Sea (C) and the Ob-Yenisei River Plume (D). DCCHO abbreviations are: Ara, arabinose; Fuc, fucose; GalN, galactosamine; Gal, galactose; GalA, galacturonic acid; GlcN, glucosamine; Glc, glucose; GlcA, glucuronic acid; Man+ Xyl, mannose + xylose; Rha, rhamnose. Colour-coded bar indicates phylum affiliation, while the blue-to-red scale reflects correlation strength. Significant correlations are highlighted according to significance levels (p-values: < 0.001 *, 0.001-0.01 **, 0.01-0.05 *, > 0.05).**

3.6 Linking protist community to carbohydrate composition

A Mantel test analysis revealed a significant correlation between phytoplankton community structure and DCCHO composition (Spearman's $r = 0.31$, $p < 0.001$). To further examine the relationship between individual indicator taxa of each region and specific monomeric sugars, we applied pairwise Spearman correlations. In the FS, the haptophyte *Phaeocystis* sp. and the diatom *Pseudo-nitzschia* sp. were strongly positively correlated with rhamnose and particularly arabinose, whereas the dinoflagellate *Heterocapsa* sp. showed weaker positive correlations with arabinose, galactose and glucose (Fig. 7B). Across all taxa, significant negative associations were observed with fucose and amino sugars. In contrast, indicator taxa in the KS were positively associated with fucose and amino sugars, including dinoflagellates of the genera *Karlodinium* and *Prorocentrum* as well as an unidentified prymnesiophyte (Fig. 7C). Only diatoms showed significant positive correlations with glucose, with *Thalassiosira* sp. exhibiting the strongest relationship, followed by *Minidiscus* sp. and *Chaetoceros* sp. *Eucampia* was the only diatom lacking a significant association with glucose but instead showed a positive correlation with galactosamine. In the RP, all indicator taxa, regardless of phylogenetic affiliation, were negatively correlated with glucose and mannose+xylose but positively associated with galactose, fucose and glucosamine and to a lesser extent with glucuronic acid (Fig. 7D). Notably, galactosamine showed no significant correlations with any taxa except for a single unidentified dinoflagellate.

4. Discussion

Our study examined how regional and seasonal differences in phytoplankton community composition are associated with the quantity and quality of DOM and the formation of TEP across contrasting Arctic sectors. Disentangling these relationships is critical to understanding how shifts in phytoplankton communities influence the balance between carbon recycling in the microbial loop and carbon export. To address this, we assessed DOM origin and diagenetic state using established biogeochemical proxies, including DOC concentrations, DCCHO composition and DOC:DON ratios (Repeta, 2015), allowing us to interpret regional patterns in organic matter sources and microbial processing within the context of bloom dynamics and hydrography.

https://doi.org/10.5194/egusphere-2026-4192
Preprint. Discussion started: 17 July 2026

4.1 Regional and seasonal phytoplankton bloom dynamics

The primary spring bloom in the FS is initiated by sea-ice retreat and increasing light availability (Cherkasheva et al., 2014). In late May to late June, we observed main bloom events in the transition zone between the WSC and the EGC, particularly at wPSW- and PSW-dominated HAUSGARTEN (HG) and northern stations (N), confirming earlier observations that spring blooms tend to develop first in polar waters before spreading into Atlantic waters (Lampe et al., 2021; 2026). Elevated chl-*a* concentrations (~2–4 µg L^{-1}) exceeded the majority of previously reported values for June to October (~1.5 µg L^{-1}; Piontek et al., 2014; Nöthig et al., 2020; von Jackowski et al., 2020). Concurrently, nitrate concentrations were substantially reduced (~3.4 and ~1.6 µmol L^{-1}) relative to winter-replenished levels (~11 µmol L^{-1}; von Appen et al., 2021). Together, the elevated chl-*a* concentrations and substantial nitrate drawdown indicate that the spring bloom already reached an advanced stage, further supported by low phytoplankton evenness and the dominance of single phytoplankton taxa (ASVs), consistent with reduced community complexity during late bloom stages.

The spring bloom community was dominated by either diatoms or haptophytes. One bloom event, confined to HG4, was strongly dominated the diatom *Chaetoceros gelidus* and occurred under partial ice coverage (~80%), which is consistent with a typical ice-edge diatom bloom (Rat'kova & Wassmann, 2002; Weiß et al., 2024). Another bloom event was characterised by high proportions of *Phaeocystis pouchetii* and frequent occurrences of the dinoflagellate genus *Gyrodinium* and the order Syndiniales. The co-occurrence of *Gyrodinium* spp., a reported grazer of *Phaeocystis* (Grattepanche et al., 2011) and Syndiniales, an order that includes many parasitic lineages known to recycle phytoplankton biomass (Clarke et al., 2019), suggests that multi-trophic interactions may have contributed to bloom dynamics and biomass turnover.

In contrast to the FS, depleted nitrate, phosphate, and silicate concentrations, alongside slightly elevated nitrite levels indicative of active microbial remineralization and nitrification (Tuerena et al., 2021), point to nutrient-limited post-bloom regime in the KS and RP. Such conditions favoured a mixotrophic, phagotrophic and bacterivorous community dominated by dinoflagellates (*Karlodinium* spp., *Gymnodinium* spp., *Gyrodinium* spp.), as well as taxa from Cryptophyceae (*Teleaulax* sp., *Hemiselmis* sp.), Chrysophyceae (*Dinobryon* spp.), and Chlorophyta (*Micromonas* spp.), characteristic of resource limitation and enhanced recycling within the microbial loop (Stoecker & Lavrentyev, 2018; Li et al., 2022). Consistently low surface chl-*a* concentrations and frequent subsurface chlorophyll *a* maxima are in accordance with previous late-summer observations for this region (Demidov et al., 2021; Bukatov et al., 2025).

The weak correspondence between chl-*a* distribution and distinct water mass boundaries suggests that bloom development was primarily governed by local-scale processes such as nutrient regeneration, and ice-edge dynamics. Exceptionally high chl-*a* concentrations (~6.5 to 8 µg L^{-1}) along the shelf break of the KS, likely related to the sea-ice edge (Fig. S8), were dominated by *Thalassiosira* spp., large cold-water diatoms commonly associated with first-year ice (Makarevich et al., 2015; Pautova et al., 2024). *Thalassiosira* spp. are typically observed during the second stage of ice-edge-bloom succession, following an initial phase dominated by small diatoms such as *Chaetoceros socialis* (Rat'kova & Wassmann, 2002). The advanced stage of this bloom is further supported by pronounced subsurface chl-*a* maxima (e.g.,

https://doi.org/10.5194/egusphere-2026-4192
Preprint. Discussion started: 17 July 2026

stations 41, 47, 67), consistent with the under-ice to ice-edge to deep open-water progression described by Mayot et al. (2018). Only station 61 showed elevated surface and subsurface chl-*a* concentrations under ~40% sea-ice cover, indicative of an ongoing ice-edge bloom.

Mesoscale hydrographic processes, including riverine inputs and Atlantic inflow, further influence phytoplankton community structure and bloom development in the KS. At shelf-edge station 57, a pronounced riverine signal from the Ob and Yenisei rivers detected in the Voronin Trough during the Arctic Century expedition (Pérez-Tribouillier et al., 2025) likely modified nutrient availability, thereby influencing phytoplankton growth conditions and subsequent DOM production and transformation. In addition, the strong influence of Barents Sea–derived Atlantic waters in the St. Anna Trough (Pérez-Tribouillier et al., 2025) coincided with an increasing contribution of *Eucampia groenlandica* at western stations. The pronounced occurrence of *E. groenlandica*, similar to recent observations linked to intensified Atlantic inflow in the Franz Victoria Trough (Pautova et al., 2024), together with the first reported appearance of *Phaeocystis* colonies in June 2021 (Sergeeva et al., 2025) and their confinement to stations along the Atlantic inflow pathway (stations 8, 13, 17, 29, 41, 47), suggests a hydrographically mediated community shift with potential implications for future DOM dynamics. Our observations highlight pronounced regional and seasonal contrasts in bloom dynamics from an advanced spring bloom in the FS, dominated by *Phaeocystis pouchetii* and *Chaetoceros gelidus*, to predominantly post-summer bloom with nutrient-recycling regimes, and punctuated by localized ice-edge and shelf-margin *Thalassiosira* spp. blooms in the KS and RP.

4.2 Contrasting DOM sources

To interpret regional differences in DOM composition, we distinguished between autochthonous DOM produced by phytoplankton and allochthonous DOM originating from terrestrial sources, as they differ markedly in composition and reactivity. Across the FS, DOM quantity and composition reflected the combined influence of hydrography and bloom dynamics. Waters influenced by the WSC exhibited lower DOC concentrations and DOC:DON ratios than PSW transported by the EGC, which carries terrigenous DOM originating from Eurasian rivers (Amon & Budéus, 2003; Engel et al., 2026). DOC concentrations were consistent with previously reported values for Atlantic (~60 µmol L^{-1}) and polar waters (79 ± 19 µmol L^{-1}) in the region (Amon et al., 2024; Engel et al., 2026), while DOC:DON ratios remained at the lower end of the regional range (10-25; Lara et al., 1998), pointing towards a substantial contribution of phytoplankton-derived DOM. Moreover, NS yields in PSW and wPSW exceeded those observed in the KS, reaching up to 19 %DOC and falling within the upper range reported for other polar marine environments (Kirchman et al., 2001; Amon & Benner, 2003; Panagiotopoulos et al., 2014). Elevated NS yields likely reflect enhanced carbohydrate exudation during active or late-stage phytoplankton blooms, when neutral sugar concentrations can increase several-fold (Obernosterer & Herndl, 1995; Kirchman et al., 2001; von Jackowski et al., 2022). Taken together, DOM composition in the FS reflects a mixed signal shaped by the interplay between advected terrestrial inputs via the EGC and spring bloom-derived marine DOM.

In the KS, comparatively low DOC concentrations and DOC:DON ratios (~10) suggest a predominantly marine DOM signal with little discernible riverine influence. This is consistent with the eastward extension of the Ob-Yenisei plume toward

https://doi.org/10.5194/egusphere-2026-4192
Preprint. Discussion started: 17 July 2026

the Vilkitsky Strait rather than into the central KS, and with Barents Sea-derived Atlantic waters influencing the St. Anna Trough surface waters (Pérez-Tribouillier et al., 2025). Low chl-*a* concentrations and amino sugar signatures, which are indicative of microbial reworking as they accumulate due to their low decay rates (Benner & Kaiser, 2003; Kawasaki & Benner, 2006), suggest that the DOM pool was already partially degraded, reaffirming post-bloom conditions (von Jackowski et al., 2022). However, elevated chl-*a* concentrations at selected stations influenced by PSW and ice showed increased NS yields (~7 %DOC), within the range reported for freshly produced phytoplankton-derived DOM (4.1-9.6 %DOC, Amon & Benner, 2003), which indicates localized inputs of labile organic matter.

In the RP, high DOC concentrations and elevated DOC:DON ratios are consistent with a strong terrestrial influence on the DOM pool, as previously observed from the Ob and Yenisei estuaries (Amon & Benner, 2003). Average DOC concentrations (~340 µmol L^{-1}) were lower than previously reported values from the river mouths (423-537 µmol L^{-1}), likely reflecting sampling near the plume margin. DOC:DON ratios of ~29 fall at the lower end of the range reported for these estuaries (29-51; Köhler et al., 2003), further suggesting partial mixing with shelf waters. Despite the predominantly terrigenous signal, NS yields were higher than typically expected for refractory terrestrial DOM (1.7–3.5 %DOC; Amon & Benner, 2003), reaching ~3.9 %DOC and up to ~5 %DOC at the easternmost stations (113, 115). These elevated yields may partly reflect the relatively high DCCHO content previously reported for the Ob and Yenisei compared with other Arctic river systems such as the Lena and Mackenzie (Kaiser et al., 2017), while the highest values at the easternmost stations may suggest additional “fresh” inputs from algal release under partial sea-ice cover.

Disentangling terrestrial and phytoplankton-derived signals in the river plume region is challenging, as both sources can contribute overlapping carbohydrate signatures. Galactose, for example, accounted for a higher proportion of carbohydrates in the RP than in the other regions, but may originate from multiple sources, including non-woody plant tissue, soil bacteria, and phytoplankton-derived organic matter (Cowie & Hedges, 1984; Biersmith & Benner, 1998; da Cuhna et al., 2002). Previously discussed DOC:DON ratios, together with very low nutrient concentrations and a predominantly mixotrophic phytoplankton community, suggest that terrestrial inputs and subsequent microbial processing exerted a stronger influence on the DOM pool than recent phytoplankton production. This is in line with Kaiser et al. (2017), who reported a comparable neutral sugar composition for the Ob and Yenisei, with galactose contributions of up to 15%, and linked the relatively uniform neutral sugar patterns across Siberian rivers to early degradation stages of plant-, soil-, and bacterially derived organic matter. A notable difference from the pattern reported by Kaiser et al. (2017) is the higher contribution of fucose relative to rhamnose in our samples, which may reflect flow-regime-related variability; however, as both sugars have been linked to bacterial reworking in river plumes, this shift may still be consistent with a microbially influenced DOM signal (Guggenberger et al., 1994; Panagiotopoulos et al., 2012). Thus, the carbohydrate signature in the RP likely reflects a mixture of terrestrial plant- and soil-derived as well as bacterially processed DOM, rather than a predominantly phytoplankton-derived source.

https://doi.org/10.5194/egusphere-2026-4192
Preprint. Discussion started: 17 July 2026

4.3 Taxonomic controls on DOM composition and implications for TEP formation

Distinct DCCHO molecular signatures across bloom types indicate taxon-associated differences in DOM quality. In the FS, *Phaeocystis*-dominated blooms were characterised by an enrichment of neutral (arabinose, rhamnose, and glucose) and acidic sugars, likely reflecting a complex heteropolysaccharide-rich DOM pool and coinciding with high TEP concentrations. These observations align with previous studies indicating that rhamnose and arabinose are major components of *Phaeocystis*-derived DOM and occur in higher relative proportions than in DOM produced by phytoplankton species from other genera (Biersmith & Benner, 1998; Aluwihare & Repeta, 1999; Alderkamp et al., 2007). Rhamnose- and arabinose-containing compounds are often associated with the production of polysaccharide-rich colonial mucus containing gel-forming acidic components. Both neutral deoxy-sugars (e.g., rhamnose and fucose) and uronic acids (e.g., glucoronic acid and galacturonic acid) have been linked to TEP formation (Alldredge et al., 1993; Skoog et al., 2008; Engel et al., 2012), with the latter playing a key role in aggregation via cation bridging (Passow, 2002; Engel et al., 2004a; Mari et al., 2005). In the present study, however, acidic sugars contributed only a minor fraction of the bloom-associated DCCHO pool (< 2 mol%), whereas previous high-TEP bloom studies reported uronic acid contributions of ~26 mol% of DCCHO in a coccolithophorid-dominated (Engel et al., 2012) and ~16 mol% of total CCHO in a diatom-dominated bloom (Sperling et al., 2017). The low abundance of acidic sugars may either reflect their rapid incorporation into TEP or indicate that acidic sugars are less dominant components of TEP produced in *Phaeocystis*-dominated systems, leaving potential taxon-specific differences in TEP composition unresolved.

In the KS, diatom-dominated blooms were characterized by a strong glucose signal alongside reduced contributions from most other sugars, indicating a simpler exopolysaccharide composition and coinciding with surprisingly low TEP concentrations. This was unexpected given the abundance of *Thalassiosira* spp., as several species within this genus are known to produce TEP precursors, although the amount released can vary among species (Burns et al. 2019). Low TEP concentrations may therefore reflect interspecies variability or additional mechanisms influencing exudation. A potential mechanism may relate to the overflow hypothesis, whereby excess fixed carbon is released when photosynthetic carbon fixation exceeds the capacity for growth under nutrient limitation (Fogg, 1966, 1983; Williams, 1990). Low nutrient conditions towards the end of the diatom bloom may therefore have favoured overflow-related glucose release, consistent with laboratory observations of nutrient-limited *Thalassiosira pseudonana* releasing carbohydrates composed almost exclusively of glucose (Urbani et al., 2005). In natural phytoplankton communities, glucose was also the dominant sugar accumulating in the DCCHO pool triggered by photosynthetic overflow (Barthelmeß et al., 2025), pointing to the importance of glucose and its role as a component of storage polysaccharides such as β-1,3-glucans in diatoms (Becker et al., 2020). Degradation of less complex polysaccharides or homopolysaccharides, composed primarily of one monomer species, requires fewer enzymatic steps and thus lower energetic investment compared to structurally complex heteropolysaccharides (Unfried et al., 2018; Sichert et al., 2020; Vidal-Melgosa et al., 2021). Thus, the pronounced enrichment of glucose could indicate a less structurally complex polysaccharide pool, which may have favoured microbial recycling over TEP formation, despite substantial carbon release.

https://doi.org/10.5194/egusphere-2026-4192
Preprint. Discussion started: 17 July 2026

5. Conclusion

In the Arctic Ocean, dissolved carbohydrate signatures and TEP dynamics varied in relation to regional hydrography, seasonal succession, and bloom identity. Distinct bloom regimes (i.e., haptophyte versus diatom dominance) were associated with contrasting DOM signatures and aggregation potential: an advanced spring bloom dominated by *Phaeocystis pouchetii* was associated with a DOM pool particularly enriched in arabinose, rhamnose, glucose and acidic sugars as well as elevated TEP concentrations, whereas localized ice-edge diatom blooms dominated by *Thalassiosira* spp. showed glucose-enriched DOM signatures indicative of simpler polysaccharides, and coinciding with comparatively low TEP formation. Under post-bloom conditions communities were characterized by mixotrophic, phagotrophic, and bacterivorous taxa, low TEP concentrations, elevated amino sugar contributions and nitrite levels, consistent with advanced DOM reworking. These observations provide direct field-based evidence that differences in phytoplankton bloom composition and stage are reflected in the molecular signature of dissolved carbohydrates and may translate into contrasting aggregation potential. The occurrence of *Eucampia groenlandica* along Atlantic inflow pathways provides further evidence for climate-induced changes such as Atlantification and their role in restructuring planktonic communities. Changes in phytoplankton community composition may alter DOM quality by favouring either structurally complex, aggregation-prone polysaccharides or less complex, more labile biopolymers, thereby influencing whether organic carbon is primarily retained in the surface waters within the microbial loop or exported to the deep ocean via TEP-mediated aggregation. To understand the potential consequences of future community shifts, further studies are needed to characterize taxon-specific polysaccharides and resolve their functional roles in TEP formation and microbial utilization.

Data availability

Environmental data will be archived in the PANGAEA World Data Centre and amplicon data will be deposited in the European Nucleotide Archive (ENA) at EMBL-EBI and is for PS126 already accessible under PRJEB108237.

Author contributions

Sophia Hirschmann: data curation, formal analysis, validation, visualization, writing - original draft, writing - review & editing. **Anabel von Jackowski**: investigation, funding acquisition, supervision, writing - review & editing. **Benjamin Pontiller**: supervision, writing - review & editing. **Katja Metfies**: investigation, resources, writing - review & editing. **Vasily Povazhnyi**: investigation. **Stefan Neuhaus**: data curation, writing - review & editing. **Eva-Maria Nöthig**: investigation, writing - review & editing. **Anja Engel**: conceptualization, funding acquisition, resources, supervision, project administration, writing - review & editing.

https://doi.org/10.5194/egusphere-2026-4192
Preprint. Discussion started: 17 July 2026

Competing interests

The authors declare no conflicts of interest.

Acknowledgements

We thank the captain and crew of the RV *Polarstern* and RV *Akademik Tryoshnikov* for their support in obtaining the samples. A special thank you to Tania Klüver, Jon Roa and Swantje Ziemann for helping with or running sample analysis in the laboratory.

Financial support

The RV Polarstern expedition was funded under AWI_PS126_02 and its 18S sample collection was supported by the framework of the HGF infrastructure program Frontiers in Arctic Marine Monitoring (FRAM). This research used samples provided by the Arctic Century expedition a joint initiative led by the Swiss Polar Institute (SPI), the Antarctic and Arctic Research Institute (AARI), and GEOMAR Helmholtz Centre for Ocean Research Kiel (GEOMAR) and funded by the Swiss Polar Foundation. Furthermore, the Swiss Polar Institute supported analyses for phytoplankton sequencing (grant ID: ARCEN-2023-004) and the dissolved combined carbohydrate (DCCHO) analysis (grant ID: ARCEN-2023-008). SH was supported by the Helmholtz Association. AvJ was supported by the Helmholtz Association and later the Marie-Curie Postdoctoral Fellowship ACUTE (grant ID: 101210310). Open-access publication fees were covered by GEOMAR.

References

Ahme, A., Von Jackowski, A., McPherson, R. A., Wolf, K. K. E., Hoppmann, M., Neuhaus, S., and John, U.: Winners and Losers of Atlantification: The Degree of Ocean Warming Affects the Structure of Arctic Microbial Communities, Genes, 14, 623, https://doi.org/10.3390/genes14030623, 2023.

Alderkamp, A. C., Buma, A. G. J., and Van Rijssel, M.: The carbohydrates of *Phaeocystis* and their degradation in the microbial food web, Biogeochemistry, 83, 99–118, https://doi.org/10.1007/s10533-007-9078-2, 2007.

Alldredge, A. L., Passow, U., and Logan, B. E.: The abundance and significance of a class of large, transparent organic particles in the ocean, Deep Sea Research Part I: Oceanographic Research Papers, 40, 1131–1140, https://doi.org/10.1016/0967-0637(93)90129-Q, 1993.

Aluwihare, L. I. and Repeta, D. J.: A comparison of the chemical characteristics of oceanic DOM and extracellular DOM produced by marine algae, Mar. Ecol. Prog. Ser., 186, 105–117, https://doi.org/https://doi.org/10.3354/meps186105, 1999.

Amon, R. M. W. and Benner, R.: Combined neutral sugars as indicators of the diagenetic state of dissolved organic matter in the Arctic Ocean, Deep-Sea Research I, 50, 151–169, https://doi.org/10.1016/S0967-0637(02)00130-9, 2003.

https://doi.org/10.5194/egusphere-2026-4192
Preprint. Discussion started: 17 July 2026

Amon, R. M. W. and Budéus, G.: Dissolved organic carbon distribution and origin in the Nordic Seas: Exchanges with the Arctic Ocean and the North Atlantic, J. Geophys. Res., 108, 3321, https://doi.org/10.1029/2002jc001594, 2003.

Amon, R. M. W., Kaiser, K., and Engel, A.: Dissolved organic matter in the Arctic Ocean, in: Biogeochemistry of Marine Dissolved Organic Matter, edited by: Hansell, D. A. and Carlson, C. A., Academic Press, Amsterdam, 693–737, https://doi.org/10.1016/8978-0-443-13858-4.00017-4, 2024.

Arrigo, K. R. and van Dijken, G. L.: Continued increases in Arctic Ocean primary production, Prog. Oceanogr., 136, 60–70, https://doi.org/10.1016/j.pocean.2015.05.002, 2015.

Azam, F.: Microbial Control of Oceanic Carbon Flux: The Plot Thickens, Science, 280, 694–696, https://doi.org/10.1126/science.280.5364.694, 1998.

Barthelmeß, T., Cristi, A., Deppeler, S., Safi, K., Sellegri, K., Law, C. S., and Engel, A.: Pronounced Diel Cycling of Dissolved Carbohydrates and Amino Acids in the Surface Ocean and across Diverse Regimes, Environ. Sci. Technol., 59, 419–429, https://doi.org/10.1021/acs.est.4c00491, 2025.

Becker, J. W., Berube, P. M., Follett, C. L., Waterbury, J. B., Chisholm, S. W., DeLong, E. F., and Repeta, D. J.: Closely related phytoplankton species produce similar suites of dissolved organic matter, Front. Microbiol., 5, 111, https://doi.org/10.3389/fmicb.2014.00111, 2014.

Becker, S., Tebben, J., Coffinet, S., Wiltshire, K., Iversen, M. H., Harder, T., Hinrichs, K.-U., & Hehemann, J.-H.: Laminarin is a major molecule in the marine carbon cycle, PNAS, 117, 6599–6607. https://doi.org/10.1073/pnas.1917001117, 2020.

Benner, R. and Kaiser, K.: Abundance of amino sugars and peptidoglycan in marine particulate and dissolved organic matter, Limnol. Oceanogr., 48, 118–128, https://doi.org/10.4319/lo.2003.48.1.0118, 2003.

Biersmith, A. and Benner, R.: Carbohydrates in phytoplankton and freshly produced dissolved organic matter, Mar. Chem., 63, 131–144, https://doi.org/https://doi.org/10.1016/S0304-4203(98)00057-7, 1998.

Bjørrisen, P. K.: Phytoplankton exudation of organic matter: Why do healthy cells do it?, Limnol. Oceanogr., 33, 151–154, https://doi.org/10.4319/lo.1988.33.1.0151, 1988.

Borchard, C. and Engel, A.: Organic matter exudation by *Emiliania huxleyi* under simulated future ocean conditions, Biogeosciences, 9, 3405–3423, https://doi.org/10.5194/bg-9-3405-2012, 2012.

Bukatov, A. A., Pavlenko, E. A., and Solovei, N. M.: Investigation of the Upper Mixed Layer Variability in the Barents and Kara Seas, PHYSICAL OCEANOGRAPHY, 32, 187–196, 2025. [original text in Russian]

Burns, W. G., Marchetti, A., and Ziervogel, K.: Enhanced formation of transparent exopolymer particles (TEP) under turbulence during phytoplankton growth, J. Plankton Res., 41, 349–361, https://doi.org/10.1093/plankt/fbz018, 2019.

Callahan, B. J., McMurdie, P. J., Rosen, M. J., Han, A. W., Johnson, A. J. A., & Holmes, S. P.: DADA2: High-resolution sample inference from Illumina amplicon data. Nature Methods, 13, 581–583, https://doi.org/10.1038/nmeth.3869, 2016.

Carlson, C. A., Bates, N. R., Ducklow, H. W., and Hansell, D. A.: Estimation of bacterial respiration and growth efficiency in the Ross Sea, Antarctica, Aquatic Microbial Ecology, 19, 229–244, https://doi.org/10.3354/ame019229, 1999.

https://doi.org/10.5194/egusphere-2026-4192
Preprint. Discussion started: 17 July 2026

Cherkasheva, A., Bracher, A., Melsheimer, C., Köberle, C., Gerdes, R., Nöthig, E. M., Bauerfeind, E., and Boetius, A.: Influence of the physical environment on polar phytoplankton blooms: A case study in the Fram Strait, Journal of Marine Systems, 132, 196–207, https://doi.org/10.1016/j.jmarsys.2013.11.008, 2014.

Clarke, L. J., Bestley, S., Bissett, A., and Deagle, B. E.: A globally distributed Syndiniales parasite dominates the Southern Ocean micro-eukaryote community near the sea-ice edge, ISME Journal, 13, 734–737, https://doi.org/10.1038/s41396-018-0306-7, 2019.

Codispoti, L. A., Kelly, V., Thessen, A., Matrai, P., Suttles, S., Hill, V., Steele, M., and Light, B.: Synthesis of primary production in the Arctic Ocean: III. Nitrate and phosphate based estimates of net community production, Prog. Oceanogr., 110, 126–150, https://doi.org/10.1016/j.pocean.2012.11.006, 2013.

Coffin, R. B., Connolly, J. P., and Harris, P. S.: Availability of dissolved organic carbon to bacterioplankton examined by oxygen utilization, Mar. Ecol. Prog. Ser., 101, 9–22, https://doi.org/10.3354/meps101009, 1993.

Cowie, G. L., & Hedges, J. I.: Carbohydrate sources in a coastal marine environment, Geochim. Cosmochim. Acta, 48, 2075–2087. https://doi.org/10.1016/0016-7037(84)90388-0, 1984.

da Cunha, L. C., Serve, L., & Blazi, J.-L.: Neutral sugars as biomarkers in the particulate organic matter of a French Mediterranean river, Org. Geochem., 33, 953–964. https://doi.org/10.1016/S0146-6380(02)00058-X, 2002.

De Cáceres, M. and Legendre, P.: Associations between species and groups of sites: Indices and statistical inference, Ecology, 90, 3566–3574. https://doi.org/10.1890/08-1823.1, 2009.

Demidov, A. B., Gagarin, V. I., Eremeeva, E. V., Artemiev, V. A., Polukhin, A. A., Shchuka, S. A., Grigoriev, A. V., Khrapko, A. N., and Flint, M. V.: Vertical Variability of Primary Production and Chlorophyll a in the Kara Sea in the Middle of Summer: Contribution of Subsurface Maxima to the Water Column Values, Oceanology, 61, 645–661, https://doi.org/10.1134/S0001437021050040, 2021.

Donlon, C. J., Martin, M., Stark, J., Roberts-Jones, J., Fiedler, E., and Wimmer, W.: The Operational Sea Surface Temperature and Sea Ice Analysis (OSTIA) system, Remote Sensing of Environment, 116, 140–158. https://doi.org/10.1016/j.rse.2010.10.017, 2012.

Edler, L.: Recommendations on methods for marine biological studies in the Baltic Sea in Phytoplankton and Chlorophyll, Baltic Marine Biologists Publication, 5, 1–38, 1979.

Eigemann, F., Rahav, E., Grossart, H. P., Aharonovich, D., Voss, M., and Sher, D.: Phytoplankton Producer Species and Transformation of Released Compounds over Time Define Bacterial Communities following Phytoplankton Dissolved Organic Matter Pulses, Appl. Environ. Microbiol., 89, https://doi.org/10.1128/aem.00539-23, 2023.

Engel, A.: The role of transparent exopolymer particles (TEP) in the increase in apparent particle stickiness (α) during the decline of a diatom bloom, J. Plankton Res., 22, 485–497, https://doi.org/10.1093/plankt/22.3.485, 2000.

Engel, A. and Galgani, L.: The organic sea-surface microlayer in the upwelling region off the coast of Peru and potential implications for air-sea exchange processes, Biogeosciences, 13, 989–1007, https://doi.org/10.5194/bg-13-989-2016, 2016.

https://doi.org/10.5194/egusphere-2026-4192
Preprint. Discussion started: 17 July 2026

Engel, A. and Händel, N.: A novel protocol for determining the concentration and composition of sugars in particulate and in high molecular weight dissolved organic matter (HMW-DOM) in seawater, Mar. Chem., 127, 180–191, https://doi.org/10.1016/j.marchem.2011.09.004, 2011.

Engel, A., Thoms, S., Riebesell, U., Rochelle-Newall, E., and Zondervan, I.: Polysaccharide aggregation as a potential sink of marine dissolved organic carbon, Nature, 428, 929–932, https://doi.org/10.1038/nature02453, 2004a.

Engel, A., Delille, B., Jacquet, S., Riebesell, U., Rochelle-Newall, E., Terbrüggen, A., and Zondervan, I.: Transparent exopolymer particles and dissolved organic carbon production by *Emiliania huxleyi* exposed to different CO2 concentrations: a mesocosm experiment, Aquatic Microbial Ecology, 34, 93–104, https://doi.org/10.3354/ame034093, 2004b.

Engel, A., Harlay, J., Piontek, J., and Chou, L.: Contribution of combined carbohydrates to dissolved and particulate organic carbon after the spring bloom in the northern Bay of Biscay (North-Eastern Atlantic Ocean), Cont. Shelf Res., 45, 42–53, https://doi.org/10.1016/j.csr.2012.05.016, 2012.

Engel, A., von Jackowski, A., Lampe, V., and Nöthig, E. M.: Time series of dissolved organic carbon in the Fram Strait (2010–2021): Indications for increased river export of DOC to the East Greenland Current?, Deep. Sea. Res. 2. Top. Stud. Oceanogr., 226, https://doi.org/10.1016/j.dsr2.2025.105586, 2026.

Evans, C. A., and O'Reily, J. E.: A Manual for Measurement of Chlorophyll *a* In Netplankton and Nannoplankton, Ocean Pulse Technical Manual No. 3, Report No. SHRL. Grand Forks, ND: BIOMASS, 80–81, https://repository.library.noaa.gov/view/noaa/47554, 1980.

Fadeev, E., Salter, I., Schourup-Kristensen, V., Nöthig, E. M., Metfies, K., Engel, A., Piontek, J., Boetius, A., and Bienhold, C.: Microbial communities in the east and west Fram strait during sea ice melting season, Front. Mar. Sci., 5, 429, https://doi.org/10.3389/fmars.2018.00429, 2018.

Falkowski, P. G., Barber, R. T., and Smetacek, V.: Biogeochemical Controls and Feedbacks on Ocean Primary Production, Science, 281, 200–206, https://doi.org/10.1126/science.281.5374.200, 1998.

Fogg, G. E.: The extracellular products of algae, Oceanography and Marine Biology: An Annual Review, 4, 195–212, 1966.

Fogg, G. E.: The ecological significance of extracellular products of phytoplankton photosynthesis, Botanica Marina, 26, 3–14, https://doi.org/10.1515/botm.1983.26.1.3, 1983.

Gangnus, I., Makhotin, M., Cherniavskaia, E., Hölemann, J. A., Kusse-Tiuz, N., Lavinen, N., Malinovskiy, S., Merkulov, V., Ruiz-Castillo, E., Viazigina, N., and Kassens, H.: Nutrients, oxygen, total alkalinity, pH, and physical oceanography measured on water bottle samples during Akademik Tryoshnikov cruise Arctic Century 2021 Expedition (AT21), Arctic Ocean, PANGAEA, https://doi.org/10.1594/PANGAEA.947808, 2022.

Good, S., Fiedler, E., Mao, C., Martin, M. J., Maycock, A., Reid, R., Roberts-Jones, J., Searle, T., Waters, J., While, J., and Worsfold, M.: The Current Configuration of the OSTIA System for Operational Production of Foundation Sea Surface Temperature and Ice Concentration Analyses, Remote Sensing, 12, 720, https://doi.org/10.3390/rs12040720, 2020.

https://doi.org/10.5194/egusphere-2026-4192
Preprint. Discussion started: 17 July 2026

Gordeev, V. V., Martin, J. M., Sidorov, I. S., and Sidorova, M. V.: A reassessment of the Eurasian river input of water, sediment, major elements, and nutrients to the Arctic Ocean, American Journal of Science, 296, 664–691, https://doi.org/10.2475/ajs.296.6.664, 1996.

Gradinger, R. R. and Baumann, M. E. M.: Distribution of phytoplankton communities in relation to the large-scale hydrographical regime in the Fram Strait, Marine Biology, 111, 311–321, https://doi.org/10.1007/BF01319714, 1991.

Granum, E., Kirkvold, S., and Myklestad, S. M.: Cellular and extracellular production of carbohydrates and amino acids by the marine diatom *Skeletonema costatum*: diel variations and effects of N depletion, Mar. Ecol. Prog. Ser., 242, 83–94, https://doi.org/https://doi.org/10.3354/meps, 2002.

Grattepanche, J. D., Vincent, D., Breton, E., and Christaki, U.: Microzooplankton herbivory during the diatom-*Phaeocystis* spring succession in the eastern English Channel, J. Exp. Mar. Biol. Ecol., 404, 87–97, https://doi.org/10.1016/j.jembe.2011.04.004, 2011.

Guggenberger, G., Christensen, B. T., and Zech, W.: Land-use effects on the composition of organic matter in particle-size separates of soil: I. Lignin and carbohydrate signature, Eur. J. Soil Sci., 45, 449–458, https://doi.org/10.1111/j.1365-2389.1994.tb00530.x, 1994.

Guillou, L., Bachar, D., Audic, S., Bass, D., Berney, C., Bittner, L., Boutte, C., Burgaud, G., de Vargas, C., Decelle, J., del Campo, J., Dolan, J. R., Dunthorn, M., Edvardsen, B., Holzmann, M., Kooistra, W. H. C. F., Lara, E., Le Bescot, N., Logares, R., Mahé F., Massana R., Montresor M., Morard R, Not F, Pawlowski J., Probert I., Sauvadet A.L., Siano R., Stoeck T., Vaulot D., Zimmermann P., Christen, R.: The Protist Ribosomal Reference database (PR2): a catalog of unicellular eukaryote Small Sub-Unit rRNA sequences with curated taxonomy, Nucleic Acids Research, 41, D597–D604, https://doi.org/10.1093/nar/gks1160, 2012.

Hansell, D. A., Carlson, C. A., Repeta, D. J., and Schlitzer, R.: Dissolved organic matter in the ocean a controversy stimulates new insights, Oceanography, 22, 202–211, https://doi.org/10.5670/oceanog.2009.109, 2009.

Hedges, J. I.: Global biogeochemical cycles: progress and problems, Mar. Chem., 39, 67–93, https://doi.org/10.1016/0304-4203(92)90096-S, 1992.

Hijmans, R. J.: *terra: Spatial Data Analysis*, CRAN: Contributed Packages, The R Foundation, https://doi.org/10.32614/cran.package.terra, 2025.

Hill, V. J., Matrai, P. A., Olson, E., Suttles, S., Steele, M., Codispoti, L. A., and Zimmerman, R. C.: Synthesis of integrated primary production in the Arctic Ocean: II. In situ and remotely sensed estimates, Prog. Oceanogr., 110, 107–125, https://doi.org/10.1016/j.pocean.2012.11.005, 2013.

Hölemann, J. A., Kusse-Tiuz, N., Ruiz-Castillo, E., Malinovskiy, S., Merkulov, V., Burkhardt, M., Makhotin, M., and Kassens, H.: Physical oceanography measured with Underway-CTD (UCTD) during Akademik Tryoshnikov cruise Arctic Century 2021 Expedition (AT21), Arctic Ocean, PANGAEA, https://doi.org/10.1594/PANGAEA.947810, 2022.

Hothorn, T., Hornik, K., van de Wiel, M. A., & Zeileis, A.: A Lego System for Conditional Inference, The American Statistician, 60, 257–263, https://doi.org/10.1198/000313006X118430, 2006.

https://doi.org/10.5194/egusphere-2026-4192
Preprint. Discussion started: 17 July 2026

Ingvaldsen, R. B., Assmann, K. M., Primicerio, R., Fossheim, M., Polyakov, I. V., and Dolgov, A. V.: Physical manifestations and ecological implications of Arctic Atlantification, Nat. Rev. Earth Environ., 2, 874–889, https://doi.org/10.1038/s43017-021-00228-x, 2021.

IOC, SCOR, and IAPSO: The international thermodynamic equation of seawater – 2010: Calculation and use of thermodynamic properties, Intergovernmental Oceanographic Commission, Manuals and Guides No. 56, UNESCO (English), 196, 2010.

Ivanov, V.V.: Presnovodnyi balans Severnogo Ledovitogo okeana (The Arctic Ocean freshwater balance), Proceedings of AARI, 323, 138–147, 1976. [in Russian]

Kaiser, K., and Benner, R.: Biochemical composition and size distribution of organic matter at the Pacific and Atlantic time-series stations, Mar. Chem., 113, 63–77, https://doi.org/10.1016/j.marchem.2008.12.004, 2009.

Kaiser, K., Canedo-Oropeza, M., McMahon, R., and Amon, R. M. W.: Origins and transformations of dissolved organic matter in large Arctic rivers, Sci. Rep., 7, 13064, https://doi.org/10.1038/s41598-017-12729-1, 2017.

Kawasaki, N. and Benner, R.: Bacterial release of dissolved organic matter during cell growth and decline: Molecular origin and composition, Limnol. Oceanogr., 51, 2170–2180, https://doi.org/10.4319/lo.2006.51.5.2170, 2006.

Kelley, D., Richards, C., and SCOR/IAPSO, W.: *gsw: Gibbs Sea Water Functions*, https://doi.org/10.32614/CRAN.package.gsw, 2024.

Kieft, B., Li, Z., Bryson, S., Hettich, R. L., Pan, C., Mayali, X., and Mueller, R. S.: Phytoplankton exudates and lysates support distinct microbial consortia with specialized metabolic and ecophysiological traits, PNAS, 118, https://doi.org/10.1073/pnas.2101178118, 2021.

Kirchman, D. L., Meon, B., Ducklow, H. W., Carlson, C. A., Hansell, D. A., Steward, G. F., and Kirchman, D. L.: Glucose fluxes and concentrations of dissolved combined neutral sugars (polysaccharides) in the Ross Sea and Polar Front Zone, Antarctica, Deep. Sea. Res. 2. Top. Stud. Oceanogr., 48, 4179–4197, https://doi.org/10.1016/S0967-0645(01)00085-6, 2001.

Köhler H, Meon B, Gordeev V.V, Spitzy A, and Amon R: Dissolved organic matter (DOM) in the estuaries of Ob and Yenisei and the adjacent Kara Sea, Russia, in: Siberian River Run-off in the Kara Sea: Characterisation, Quantification, Variability & Environmental Significance, edited by: Stein, R., Fahl, K., Futterer, D. K., Galimov, E. M., and Stepanets, O. V., Elsevier Science B.V., Amsterdam, 281–308, 2003.

Lampe, V., Nöthig, E. M., and Schartau, M.: Spatio-Temporal Variations in Community Size Structure of Arctic Protist Plankton in the Fram Strait, Front. Mar. Sci., 7, https://doi.org/10.3389/fmars.2020.579880, 2021.

Lampe, V., Oschlies, A., and Schartau, M.: Differences in bloom phenology and seasonal chlorophyll-*a* variability in the Fram Strait's hydrographic subregions resolved by a machine learning approach, Deep. Sea. Res. 2. Top. Stud. Oceanogr., 226, https://doi.org/10.1016/j.dsr2.2026.105603, 2026.

https://doi.org/10.5194/egusphere-2026-4192
Preprint. Discussion started: 17 July 2026

Lara, R. J., Rachold, V., Kattner, G., Hubberten, H. W., Guggenberger, G., Skoog, A., and Thomas, D. N.: Dissolved organic matter and nutrients in the Lena River, Siberian Arctic: Characteristics and distribution, Mar. Chem., 59, 301–309, https://doi.org/10.1016/S0304-4203(97)00076-5, 1998.

Lewis, K. M., Van Dijken, G. L., and Arrigo, K. R.: Changes in phytoplankton concentration now drive increased Arctic Ocean primary production, Science, 369, 198–202, https://doi.org/10.1126/science.aay8380, 2020.

Li, M., Chen, Y., Zhang, F., Song, Y., Glibert, P. M., and Stoecker, D. K.: A three-dimensional mixotrophic model of Karlodinium veneficum blooms for a eutrophic estuary, Harmful Algae, 113, https://doi.org/10.1016/j.hal.2022.102203, 2022.

Lønborg, C., Middelboe, M., and Brussaard, C. P. D.: Viral lysis of *Micromonas pusilla*: impacts on dissolved organic matter production and composition, Biogeochemistry, 116, 231–240, https://doi.org/10.1007/s10533-013-9853-1, 2013.

Maechler, M., Rousseeuw, P., Struyf, A., Hubert, M., and Hornik, K.: cluster: Cluster Analysis Basics and Extensions, https://doi.org/10.32614/CRAN.package.cluster, 2023.

Makarevich, P. R., Larionov, V. V., and Moiseev, D. V.: Phytoplankton succession in the Ob-Yenisei Shallow zone of the Kara Sea based on Russian databases, J. Sea Res., 101, 31–40, https://doi.org/10.1016/j.seares.2014.10.008, 2015.

Makhotin, M., Hölemann, J. A., Kusse-Tiuz, N., Ruiz-Castillo, E., Malinovskiy, S., Merkulov, V., Burkhardt, M., and Kassens, H.: Physical oceanography (CTD/Rosette) during Akademik Tryoshnikov cruise Arctic Century 2021 Expedition (AT21), Arctic Ocean, PANGAEA, https://doi.org/10.1594/PANGAEA.947953, 2022.

Mari, X.: Carbon content and C:N ratio of transparent exopolymeric particles (TEP) produced by bubbling exudates of diatoms, Mar. Ecol. Prog. Ser., 183, 59–71, https://doi.org/10.3354/meps183059, 1999.

Mari, X., Rassoulzadegan, F., Brussaard, C. P. D., and Wassmann, P.: Dynamics of transparent exopolymeric particles (TEP) production by *Phaeocystis globosa* under N- or P-limitation: a controlling factor of the retention/export balance, Harmful Algae, 4, 895–914, https://doi.org/10.1016/j.hal.2004.12.014, 2005.

Martin, M.: Cutadapt removes adapter sequences from high-throughput sequencing reads, EMBnet.Journal, 17, 10, https://doi.org/10.14806/ej.17.1.200, 2011.

Mayot, N., Matrai, P., Ellingsen, I. H., Steele, M., Johnson, K., Riser, S. C., and Swift, D.: Assessing Phytoplankton Activities in the Seasonal Ice Zone of the Greenland Sea Over an Annual Cycle, J. Geophys. Res. Oceans, 123, 8004–8025, https://doi.org/10.1029/2018JC014271, 2018.

McClelland, J. W., Déry, S. J., Peterson, B. J., Holmes, R. M., and Wood, E. F.: A pan-arctic evaluation of changes in river discharge during the latter half of the 20th century, Geophys. Res. Lett., 33, https://doi.org/10.1029/2006GL025753, 2006.

McKnight, D. T., Huerlimann, R., Bower, D. S., Schwarzkopf, L., Alford, R. A., and Zenger, K. R.: microDecon: A highly accurate read-subtraction tool for the post-sequencing removal of contamination in metabarcoding studies, Environmental DNA, 1, 14–25, https://doi.org/10.1002/edn3.11, 2019.

https://doi.org/10.5194/egusphere-2026-4192
Preprint. Discussion started: 17 July 2026

Meyer, A., Sundfjord, A., Fer, I., Provost, C., Villacieros Robineau, N., Koenig, Z., Onarheim, I. H., Smedsrud, L. H., Duarte, P., Dodd, P. A., Graham, R. M., Schmidtko, S., and Kauko, H. M.: Winter to summer oceanographic observations in the Arctic Ocean north of Svalbard. J. Geophys. Res. Oceans, 122, 6218–6237, https://doi.org/10.1002/2016JC012391, 2017.

Møller, E. F.: Production of dissolved organic carbon by sloppy feeding in the copepods *Acartia tonsa*, *Centropages typicus*, and *Temora longicornis*, Limnol. Oceanogr., 52, 79–84, https://doi.org/10.4319/lo.2007.52.1.0079, 2007.

Nöthig, E. M., Bracher, A., Engel, A., Metfies, K., Niehoff, B., Peeken, I., Bauerfeind, E., Cherkasheva, A., Gäbler-Schwarz, S., Hardge, K., Kilias, E., Kraft, A., Kidane, Y. M., Lalande, C., Piontek, J., Thomisch, K., and Wurst, M.: Summertime plankton ecology in fram strait-a compilation of long-and short-term observations, Polar Res., 34, 23349, https://doi.org/10.3402/polar.v34.23349, 2015.

Nöthig, E. M., Ramondenc, S., Haas, A., Hehemann, L., Walter, A., Bracher, A., Lalande, C., Metfies, K., Peeken, I., Bauerfeind, E., and Boetius, A.: Summertime Chlorophyll *a* and Particulate Organic Carbon Standing Stocks in Surface Waters of the Fram Strait and the Arctic Ocean (1991–2015), Front. Mar. Sci., 7, https://doi.org/10.3389/fmars.2020.00350, 2020.

Obernosterer, I. and Herndl, G. J.: Phytoplankton extracellular release and bacterial growth: dependence on the inorganic N:P ratio, Mar. Ecol. Prog. Ser., 166, 247–257, https://doi.org/10.3354/meps116247, 1995.

Oksanen, J., Simpson, G. L., Blanchet, F. G., Kindt, R., Legendre, P., Minchin, P. R., O'Hara, R. B., Solymos, P., Stevens, M. H. H., Szoecs, E., Wagner, H., Barbour, M., Bedward, M., Bolker, B., Borcard, D., Carvalho, G., Chirico, M., De Caceres, M., Durand, S., Evangelista H, FitzJohn R, Friendly M, Furneaux B, Hannigan G, Hill M, Lahti L, McGlinn D, Ouellette M, Ribeiro Cunha E, Smith T, Stier A, Ter Braak C, and Weedon, J.: vegan: Community Ecology Package. https://CRAN.R-project.org/package=vegan, 2024.

Osadchiev, A., Viting, K., Frey, D., Demeshko, D., Dzhamalova, A., Nurlibaeva, A., Gordey, A., Krechik, V., Spivak, E., Semiletov, I., and Stepanova, N.: Structure and Circulation of Atlantic Water Masses in the St. Anna Trough in the Kara Sea. Front. Mar. Sci., 9, https://doi.org/10.3389/fmars.2022.915674, 2022.

Pakulski, J. D. and Benner, R.: Abundance and distribution of carbohydrates in the ocean, Limnol. Oceanogr., 39, 930–940, https://doi.org/10.4319/lo.1994.39.4.0930, 1994.

Panagiotopoulos, C., Sempéré, R., Jacq, V., and Charrière, B.: Composition and distribution of dissolved carbohydrates in the Beaufort Sea Mackenzie margin (Arctic Ocean), Mar. Chem., 166, 92–102, https://doi.org/10.1016/j.marchem.2014.09.004, 2014.

Panagiotopoulos, C., Sempéré, R., Para, J., Raimbault, P., Rabouille, C., & Charrière, B.: The composition and flux of particulate and dissolved carbohydrates from the Rhone River into the Mediterranean Sea, Biogeosciences, 9, 1827–1844, https://doi.org/10.5194/bg-9-1827-2012, 2012.

Passow, U.: Formation of transparent exopolymer particles, TEP, from dissolved precursor material, Mar. Ecol. Prog. Ser., 192, 1–11, https://doi.org/10.3354/meps192001, 2000.

https://doi.org/10.5194/egusphere-2026-4192
Preprint. Discussion started: 17 July 2026

Passow, U.: Transparent exopolymer particles (TEP) in aquatic environments, Prog. Oceanogr., 55, 287–333, https://doi.org/10.1016/S0079-6611(02)00138-6, 2002.

Passow, U. and Alldredge, A. L.: A dye-binding assay for the spectrophotometric measurement of transparent exopolymer particles (TEP), Limnol. Oceanogr., 40, 1326–1335, https://doi.org/10.4319/lo.1995.40.7.1326, 1995.

Pautova, L., Kravchishina, M., Silkin, V., Klyuvitkin, A., Chultsova, A., Vazyulya, S., Glukhovets, D., and Artemyev, V.: The Influence of the Atlantic Water Boundary Current on the Phytoplankton Composition and Biomass in the Northern Barents Sea and the Adjacent Nansen Basin, J. Mar. Sci. Eng., 12, 1678, https://doi.org/10.3390/jmse12091678, 2024.

Pérez-Tribouillier, H., Jaccard, S. L., Blaser, P., Christl, M., Creac'h, L., Hölemann, J., Scheiwiller, M., Vockenhuber, C., Wefing, A. M., and Casacuberta, N.: The Role of the St. Anna Trough in Atlantic Water Transport Into the Arctic Ocean: A Novel Radiogenic Isotope Assessment Using Iodine, Uranium, and Neodymium, J. Geophys. Res. Oceans, 130, https://doi.org/10.1029/2024JC022050, 2025.

Peterson, B. J., Holmes, R. M., McClelland, J. W., Vörösmarty, C. J., Lammers, R. B., Shiklomanov, A. I., Shiklomanov, I. A., and Rahmstorf, S.: Increasing River Discharge to the Arctic Ocean, Science, 298, 2171–2173, https://doi.org/10.1126/science.1077445, 2002.

Piontek, J., Sperling, M., Nöthig, E.-M., and Engel, A.: Regulation of bacterioplankton activity in Fram Strait (Arctic Ocean) during early summer: The role of organic matter supply and temperature, J. Marine Syst., 132, 83–94, https://doi.org/10.1016/j.jmarsys.2014.01.003, 2014.

Pivovarov, S., Schlitzer, R., and Novikhin, A.: River run-off influence on the water mass formation in the Kara Sea, in: Siberian River Run-off in the Kara Sea: Characterisation, Quantification, Variability & Environmental Significance, edited by: Stein, R., Fahl, K., Futterer, D. K., Galimov, E. M., and Stepanets, O. V., Elsevier Science B.V., Amsterdam, 9–26, 2003.

Prakash, G., Rajula, G. R., & Sarma, V. V. S. S.: Role of phytoplankton composition on exudation of dissolved organic carbon in the Bay of Bengal, Cont. Shelf Res., 279, 105296, https://doi.org/10.1016/j.csr.2024.105296, 2024.

Rantanen, M., Karpechko, A. Yu., Lipponen, A., Nordling, K., Hyvärinen, O., Ruosteenoja, K., Vihma, T., and Laaksonen, A.: The Arctic has warmed nearly four times faster than the globe since 1979, Commun. Earth Environ., 3, 168, https://doi.org/10.1038/s43247-022-00498-3, 2022.

Rat'kova, T. N. and Wassmann, P.: Seasonal variation and spatial distribution of phyto- and protozooplankton in the central Barents Sea, Journal of Marine Systems, 38, 47–75, https://doi.org/10.1016/S0924-7963(02)00169-0, 2002.

Repeta, D. J.: Chemical Characterization and Cycling of Dissolved Organic Matter, in: Biogeochemistry of Marine Dissolved Organic Matter (Second Edition), edited by: Hansell, D. A. and Carlson, C. A., Academic Press, Amsterdam, 21–63, https://doi.org/10.1016/B978-0-12-405940-5.00002-9, 2015.

Rubin, B. E. R., Sanders, J. G., Hampton-Marcell, J., Owens, S. M., Gilbert, J. A., & Moreau, C. S.: DNA extraction protocols cause differences in 16S rRNA amplicon sequencing efficiency but not in community profile composition or structure, MicrobiologyOpen, 3, 910–921, https://doi.org/10.1002/mbo3.216, 2014.

https://doi.org/10.5194/egusphere-2026-4192
Preprint. Discussion started: 17 July 2026

Rudels, B.: Arctic Ocean Circulation, in: Encyclopedia of Ocean Sciences, edited by: Steele, J. H., Thorpe, S. A., and Turekian, K. K., Academic Press, Boston, 211–225, https://doi.org/10.1016/B978-012374473-9.00601-9, 2009.

Rudels, B., Meyer, R., Fahrbach, E., Ivanov, V. V., Østerhus, S., Quadfasel, D., Schauer, U., Tverberg, V., and Woodgate, R. A.: Water mass distribution in Fram Strait and over the Yermak Plateau in summer 1997, Annales Geophysicae, 18, 687–705, https://doi.org/10.1007/s00585-000-0687-5, 2000.

Schauer, U., Loeng, H., Rudels, B., Ozhigin, V. K., and Dieck, W.: Atlantic Water flow through the Barents and Kara Seas, Deep Sea Research Part I: Oceanographic Research Papers, 49, 2281–2298, https://doi.org/10.1016/S0967-0637(02)00125-5, 2002.

Sergeeva, V. M., Stepanova, S. V., Flint, M. V., Sukhanova, I. N., Fedorov, A. V., and Artemiev, V. A.: Spatial and seasonal variability of Arctic phytoplankton communities in conditions of interaction with Atlantic origin waters in the St. Anna Trough (Kara Sea), Journal of Marine Systems, 249, https://doi.org/10.1016/j.jmarsys.2025.104051, 2025.

Sharp, J. H.: Excretion of organic matter by marine phytoplankton: Do healthy cells do it?, Limnol. Oceanogr., 22, 381–399, https://doi.org/10.4319/lo.1977.22.3.0381, 1977.

Sichert, A., Corzett, C. H., Schechter, M. S., Unfried, F., Markert, S., Becher, D., Fernandez-Guerra, A., Liebeke, M., Schweder, T., Polz, M. F., and Hehemann, J.-H.: Verrucomicrobia use hundreds of enzymes to digest the algal polysaccharide fucoidan, Nature Microbiology, 5, 1026–1039, https://doi.org/10.1038/s41564-020-0720-2, 2020.

Skoog, A., Alldredge, A., Passow, U., Dunne, J., and Murray, J.: Neutral aldoses as source indicators for marine snow, Mar. Chem., 108, 195–206, https://doi.org/10.1016/j.marchem.2007.11.008, 2008.

Sperling, M., Piontek, J., Engel, A., Wiltshire, K. H., Niggemann, J., Gerdts, G., and Wichels, A.: Combined carbohydrates support rich communities of particle-associated marine bacterioplankton, Front. Microbiol., 8, https://doi.org/10.3389/fmicb.2017.00065, 2017.

Stark, J. D., Donlon, C. J., Martin, M. J., and McCulloch, M. E.: OSTIA: An operational, high resolution, real time, global sea surface temperature analysis system, OCEANS 2007-Europe, 1–4, https://doi.org/10.1109/OCEANSE.2007.4302251, 2007.

Stoecker, D. K. and Lavrentyev, P. J.: Mixotrophic plankton in the polar seas: A pan-Arctic review, Front. Mar. Sci., 5, https://doi.org/10.3389/fmars.2018.00292, 2018.

Strom, S. L., Benner, R., Ziegler, S., and Dagg, M. J.: Planktonic grazers are a potentially important source of marine dissolved organic carbon, Limnol. Oceanogr., 42, 1364–1374, https://doi.org/10.4319/lo.1997.42.6.1364, 1997.

Sumner, M.: *tidync: A Tidy Approach to "NetCDF" Data Exploration and Extraction*, https://CRAN.R-project.org/package=tidync, 2024.

Terhaar, J., Lauerwald, R., Regnier, P., Gruber, N., and Bopp, L.: Around one third of current Arctic Ocean primary production sustained by rivers and coastal erosion, Nat. Commun., 12, 169, https://doi.org/10.1038/s41467-020-20470-z, 2021.

https://doi.org/10.5194/egusphere-2026-4192
Preprint. Discussion started: 17 July 2026

Tesi, T., Muschitiello, F., Mollenhauer, G., Miserocchi, S., Langone, L., Ceccarelli, C., Panieri, G., Chiggiato, J., Nogarotto, A., Hefter, J., Ingrosso, G., Giglio, F., Giordano, P., and Capotondi, L.: Rapid Atlantification along the Fram Strait at the beginning of the 20th century, Sci. Adv., 7, https://doi.org/10.1126/sciadv.abj2946, 2021.

Thornton, D. C. O.: Dissolved organic matter (DOM) release by phytoplankton in the contemporary and future ocean, Eur. J. Phycol., 49, 20–46, https://doi.org/10.1080/09670262.2013.875596, 2014.

Tippenhauer, S., Hoppmann, M., McPherson, R., and Soltwedel, T.: Raw data of physical oceanography during RV POLARSTERN cruise PS126, PANGAEA, https://doi.org/10.1594/PANGAEA.940754, 2023.

Toseland, A., Daines, S. J., Clark, J. R., Kirkham, A., Strauss, J., Uhlig, C., Lenton, T. M., Valentin, K., Pearson, G. A., Moulton, V., and Mock, T.: The impact of temperature on marine phytoplankton resource allocation and metabolism, Nat. Clim. Chang., 3, 979–984, https://doi.org/10.1038/nclimate1989, 2013.

Tuerena, R. E., Mahaffey, C., Henley, S. F., De La Vega, C., Norman, L., Brand, T., Sanders, T., Debyser, M., Dähnke, K., Braun, J., and März, C.: Nutrient pathways and their susceptibility to past and future change in the Eurasian Arctic Ocean, Ambio, 51, 355–369, https://doi.org/10.1007/s13280-021-01673-0, 2022.

Unfried, F., Becker, S., Robb, C. S., Hehemann, J. H., Markert, S., Heiden, S. E., Hinzke, T., Becher, D., Reintjes, G., Krüger, K., Avcı, B., Kappelmann, L., Hahnke, R. L., Fischer, T., Harder, J., Teeling, H., Fuchs, B., Barbeyron, T., Amann, R. I., and Schweder, T.: Adaptive mechanisms that provide competitive advantages to marine bacteroidetes during microalgal blooms, ISME Journal, 12, 2894–2906, https://doi.org/10.1038/s41396-018-0243-5, 2018.

Urbani, R., Magaletti, E., Sist, P., and Cicero, A. M.: Extracellular carbohydrates released by the marine diatoms *Cylindrotheca closterium*, *Thalassiosira pseudonana* and *Skeletonema costatum*: Effect of P-depletion and growth status, Science of the Total Environment, 353, 300–306, https://doi.org/10.1016/j.scitotenv.2005.09.026, 2005.

Verdugo, P., Alldredge, A. L., Azam, F., Kirchman, D. L., Passow, U., and Santschi, P. H.: The oceanic gel phase: A bridge in the DOM-POM continuum, Mar. Chem., 92, 67–85, https://doi.org/10.1016/j.marchem.2004.06.017, 2004.

Vidal-Melgosa, S., Sichert, A., Francis, T. Ben, Bartosik, D., Niggemann, J., Wichels, A., Willats, W. G. T., Fuchs, B. M., Teeling, H., Becher, D., Schweder, T., Amann, R., and Hehemann, J. H.: Diatom fucan polysaccharide precipitates carbon during algal blooms, Nat. Commun., 12, 1150, https://doi.org/10.1038/s41467-021-21009-6, 2021.

von Appen, W., Wekerle, C., Hehemann, L., Schourup-Kristensen, V., Konrad, C., and Iversen, M. H.: Observations of a Submesoscale Cyclonic Filament in the Marginal Ice Zone, Geophys. Res. Lett., 45, 6141–6149, https://doi.org/10.1029/2018GL077897, 2018.

von Appen, W. J., Waite, A. M., Bergmann, M., Bienhold, C., Boebel, O., Bracher, A., Cisewski, B., Hagemann, J., Hoppema, M., Iversen, M. H., Konrad, C., Krumpen, T., Lochthofen, N., Metfies, K., Niehoff, B., Nöthig, E. M., Purser, A., Salter, I., Schaber, M., Scholz, D., Soltwedel, T., Torres-Valdes, S., Wekerle, C., Wenzhöfer, F., Wietz, M., and Boetius, A.: Sea-ice derived meltwater stratification slows the biological carbon pump: results from continuous observations, Nat. Commun., 12, 7309, https://doi.org/10.1038/s41467-021-26943-z, 2021.

https://doi.org/10.5194/egusphere-2026-4192
Preprint. Discussion started: 17 July 2026

von Jackowski, A., Grosse, J., Nöthig, E. M., and Engel, A.: Dynamics of organic matter and bacterial activity in the Fram Strait during summer and autumn: DOM and Bacteria in Fram Strait, Philos. Trans. A Math. Phys. Eng. Sci., 378, https://doi.org/10.1098/rsta.2019.0366, 2020.

von Jackowski, A., Becker, K. W., Wietz, M., Bienhold, C., Zäncker, B., Nöthig, E. M., and Engel, A.: Variations of microbial communities and substrate regimes in the eastern Fram Strait between summer and fall, Environ. Microbiol., 24, 4124–4136, https://doi.org/10.1111/1462-2920.16036, 2022.

Wangensteen, O. S. and Turon, X.: Metabarcoding Techniques for Assessing Biodiversity of Marine Animal Forests, in: Marine Animal Forests, edited by: Rossi, S., Bramanti, L., Gori, A., Orejas, C., Springer, Cham, 1–29, https://doi.org/10.1007/978-3-319-17001-5_53-1, 2016.

Wang, Q., Garrity, G. M., Tiedje, J. M., and Cole, J. R.: Naïve Bayesian Classifier for Rapid Assignment of rRNA Sequences into the New Bacterial Taxonomy, Appl. Environ. Microbiol., 73, 5261–5267, https://doi.org/10.1128/AEM.00062-07, 2007.

Weiß, J. F., von Appen, W. J., Niehoff, B., Hildebrand, N., Graeve, M., Neuhaus, S., Bracher, A., Nöthig, E. M., and Metfies, K.: Unprecedented insights into extents of biological responses to physical forcing in an Arctic sub-mesoscale filament by combining high-resolution measurement approaches, Sci. Rep., 14, 8192, https://doi.org/10.1038/s41598-024-58511-y, 2024.

Wickham, H.: *ggplot2: Elegant Graphics for Data Analysis* (Second Edition), Springer-Verlag, New York, https://doi.org/10.1007/978-3-319-24277-4, 2016.

Williams, P. J. L. B.: The importance of losses during microbial growth: commentary on the physiology, measurement and ecology of the release of dissolved organic material, Marine Microbial Food Webs, 4, 175–206, 1990.

Xi, H., Bretagnon, M., Mehdipour, E., Demaria, J., Mangin, A., and Bracher, A.: Consistent long-term observations of surface phytoplankton functional types from space, State of the Planet, 6-osr9, https://doi.org/10.5194/sp-6-osr9-7-2025, 2025.